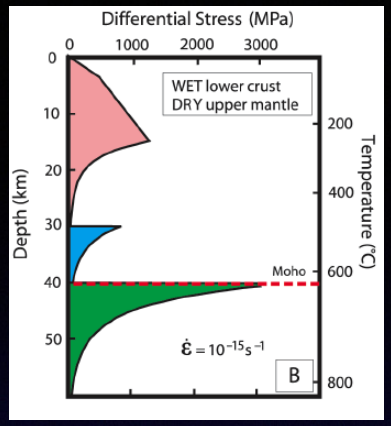

Strength and Tectonics: Brittle Deformation

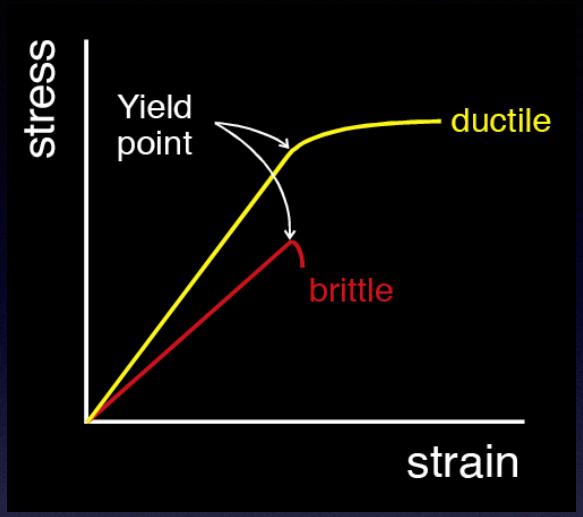

- What defines a strength profile?
  - Brittle deformation (low T, P)
  - Viscous flow laws (T, P, ...)
- Strength and Continental Kinematics
  - Oregon
  - Tibet
- Byerlee's Law, Modes of Failure, Mohr's Circles,

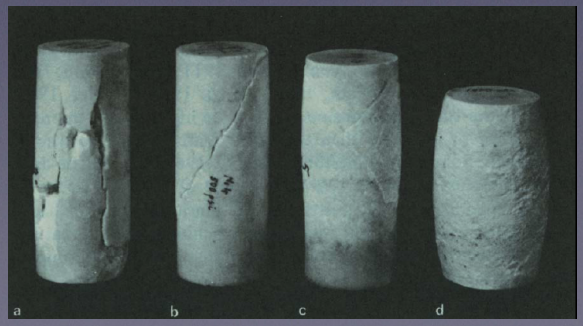

Jelly Sandwich vs. Creme Brulée

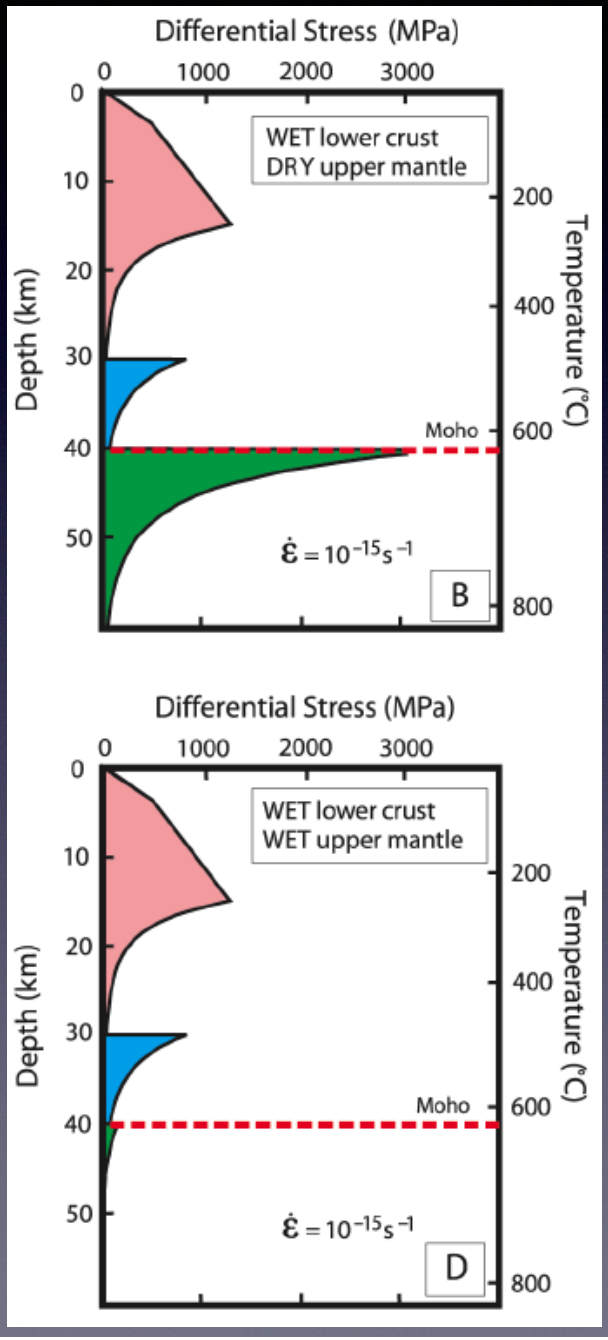

Jelly Sandwich (e.g., Chen and Molnar)

"If significant strength resides only in the seismogenic layer of the continental lithosphere, it would not be surprising if regional patterns of active faulting at the surface were dominated by the strength of the crustal blocks and the interactions between them. The strength of the faults themselves is then presumably a limiting factor in crustal behavior, but remains very uncertain." [Jackson, 2002]

Creme Brulée (e.g., Jackson)

Today we are primarily talking about continents: Oceanic lithosphere is stronger

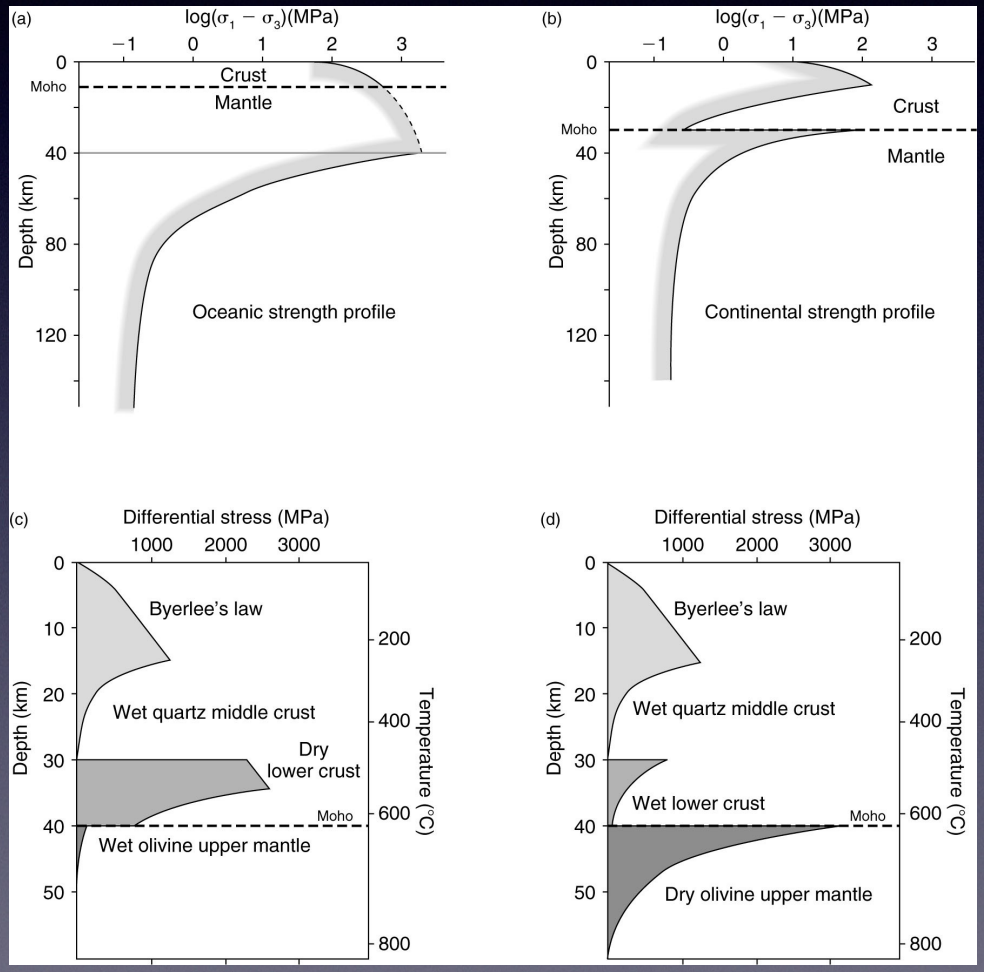

Continental Tectonics: Viscous Flow?

- Continent Deforms ~uniformly, broadly distributed =>viscous (England & McKenzie, 1982; Jackson & McKenzie, 1983; Molnar, 1988; Jackson & Molnar, 1990; England & Molnar, 1997, 2005; Holt et al., 2001; Bourne et al., 1998)
  - Upper mantle is strong
  - Crust comparatively weak
  - Crustal block interactions not important
  - Crustal motion and deformation controlled by coupling to upper mantle

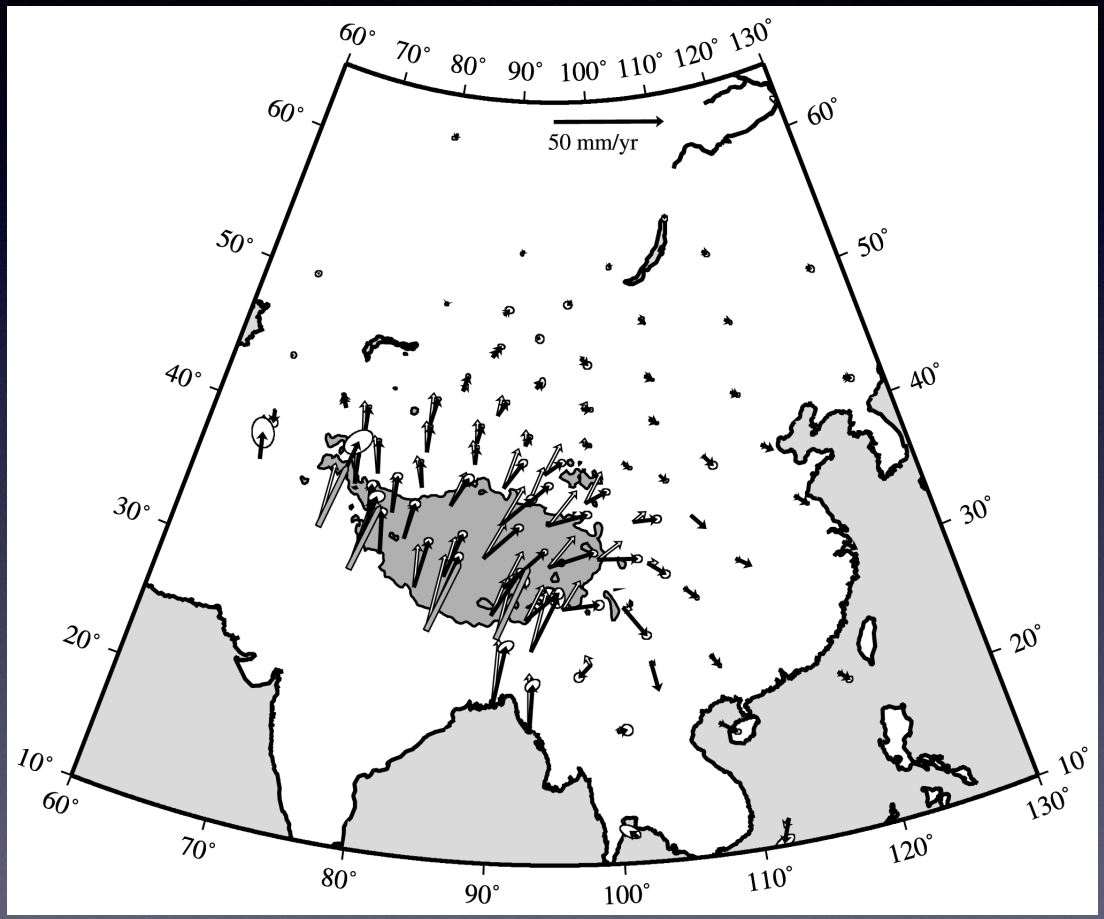

England & Molnar, 2005

Continental Tectonics: Block Interactions?

- Continent Deforms as a collection of rigid blocks (Thatcher, 1995, 2006; Jackson, 2002)
  - Upper mantle may not be strong
  - Crust is strong
  - Crustal block interactions ARE important
  - Crustal motion and deformation controlled by coupling to other blocks, with upper mantle coupling optional

JOURNAL OF GEOPHYSICAL RESEARCH, VOL. 112, B01401, doi:10.1029/2005JB004244, 2007

Click Here for Full Article

Microplate model for the present-day deformation of Tibet

Wayne Thatcher[1]

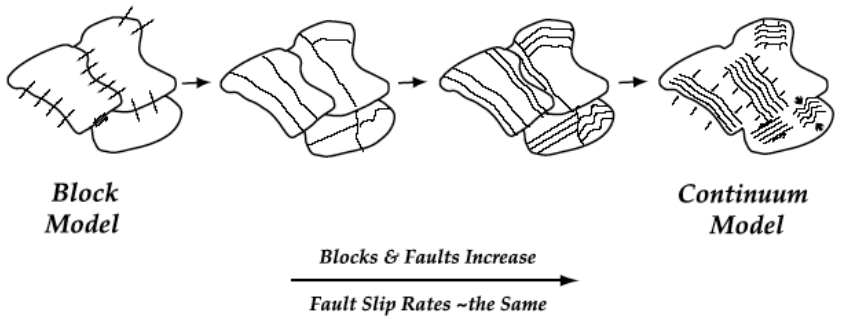

Figure 1. Schematic cartoon of end-member kinematic models for continental deformation with possible transitions from one to the other.

An even newer view, one dominated by the role of faults between blocks

"It continues to be a question of much debate as to whether the overall style of continental deformation is governed by the properties and activity of discrete, weakened shear zones or by the bulk rheological properties of the viscously deforming lower lithosphere."

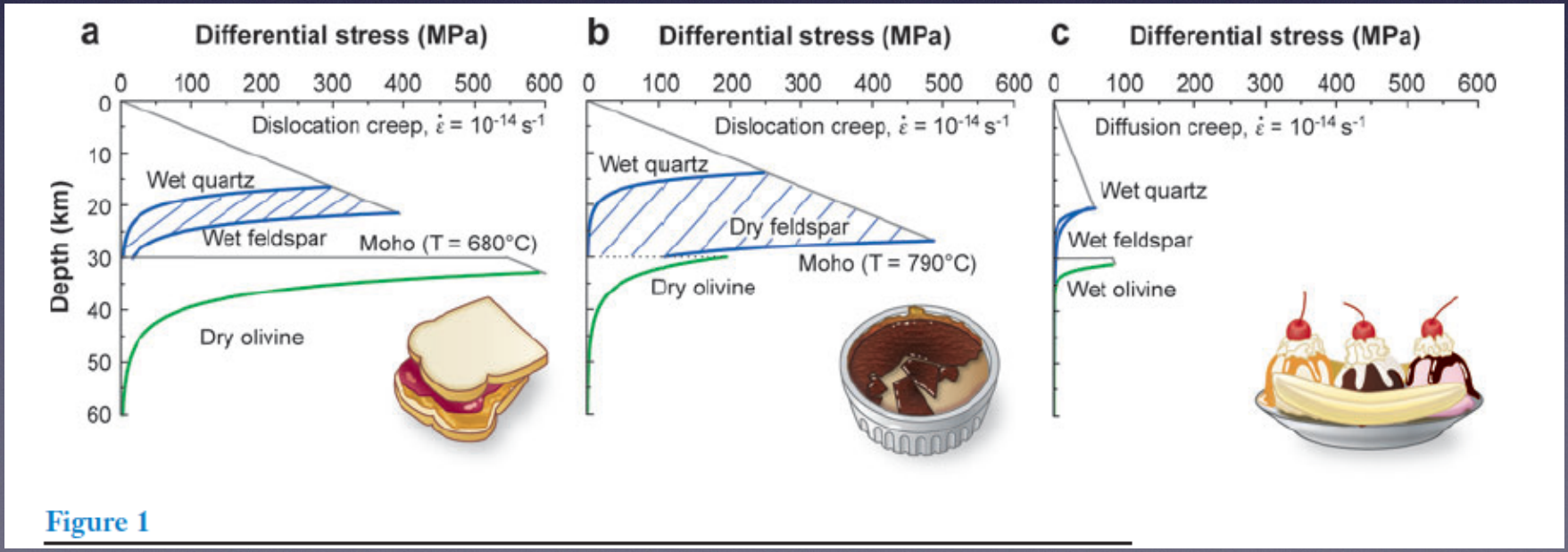

Figure 1

SUMMARY POINTS

1. Robust constitutive equations exist for major constituents of the lower crust and upper mantle that appear consistent with field and geophysical observations. Viscosity estimates based on extrapolated laboratory data for pyroxenites, dunites, anorthosites, and quartzites deformed at hydrous conditions likely span the full range of flow strengths of rocks with a more complex mineralogical composition.
2. Lithospheric strength and rheology strongly differ as a function of the makeup, tectonic evolution, and environment of a region. Thus, rheology strongly varies with depth and across continental lithosphere of varying age, composition, and temperature. Competing simple models of lithosphere rheology should be considered as end-member cases only.
3. In backarc and former backarc regions, the upper mantle is viscously weaker than the lower crust owing to high temperatures and possibly the addition of water. Mantle below old cratonic shields is an order of magnitude stronger than that found in tectonically active regions.
4. Mature fault zones are weak, and deformation along them is localized to varying degrees throughout the lithosphere. The strength of the crust below seismogenic fault zones is weakened through earthquake-cycle effects and other strain weakening processes. Strain weakening up to several orders of magnitude and localization are ubiquitous at all scales.
5. Deformation in the uppermost mantle can also localize into mylonitic shear zones, but is probably more broadly distributed in the upper-mantle asthenosphere, in which it probably occurs by dislocation creep with a stress-dependent power-law rheology.
6. Deformation mechanisms and rheology depend on thermodynamic conditions, material parameters, and mechanical state and can vary over short distance scales (inside versus outside of a shear zone) and timescales (earthquake-cycle).

Driven from Below or from Sides

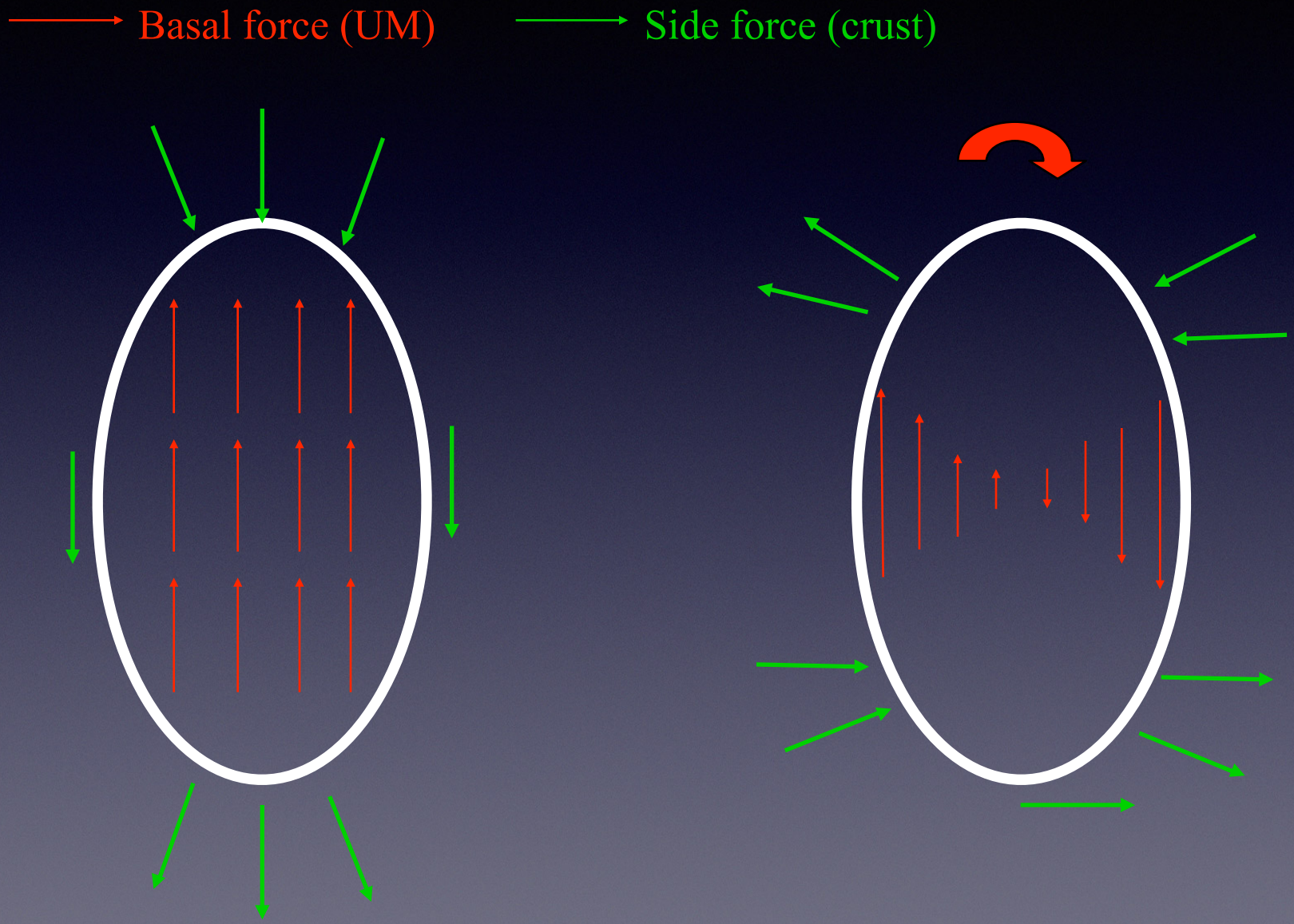

(e.g., Bourne et al., 1998)

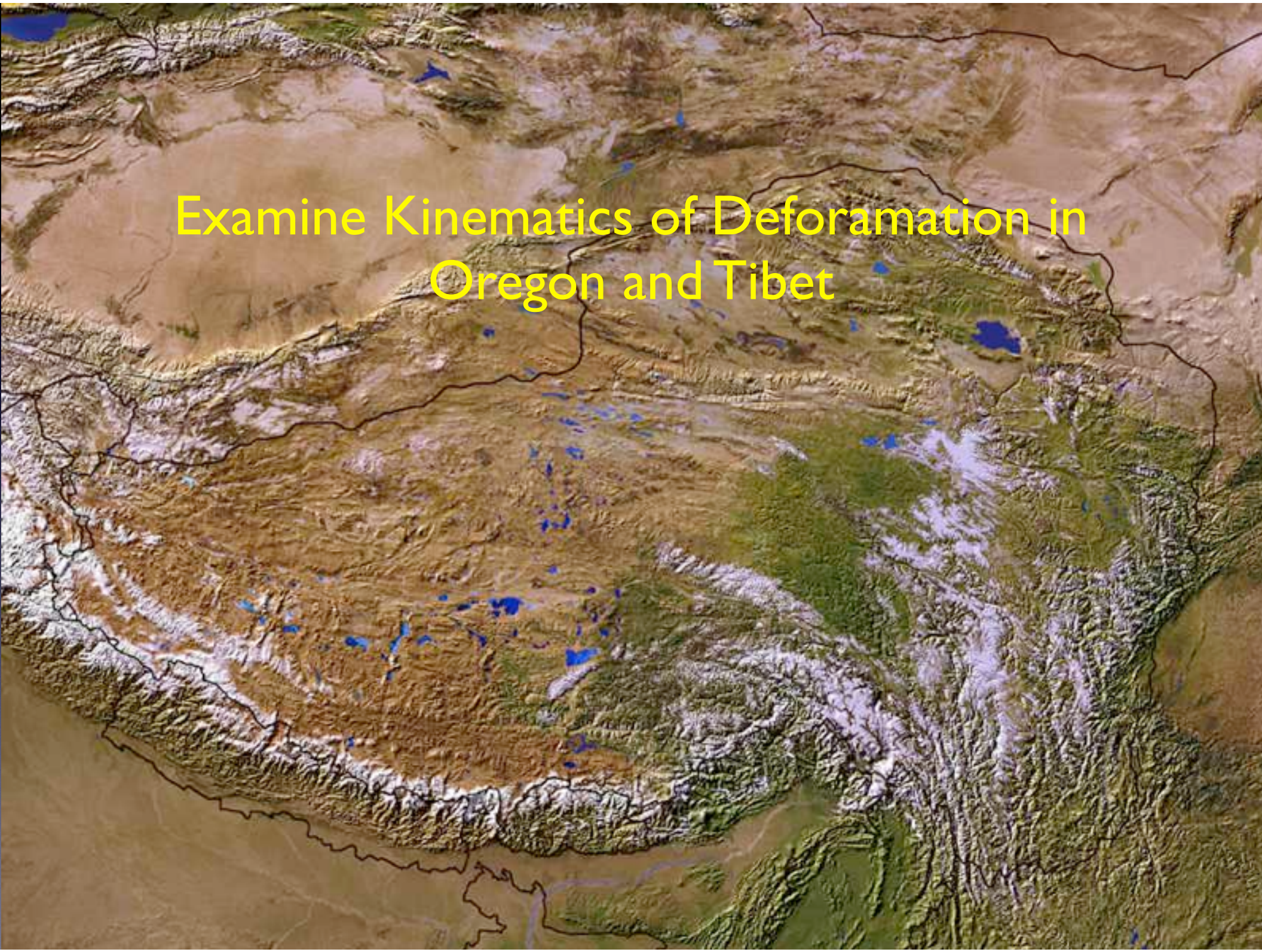
Examine Kinematics of Deforamation in
Oregon and Tibet

- Fore arc lies between megathrust and volcanic arc
- Sierra Nevada block
- Oregon block (Siletzia)
- Washington segment
- Canadian 'Buttress' (VLBI data indicate no movement wrt NA)
- Differential movement btw SN and Canada taken up by CW rotation of OC and compression of W

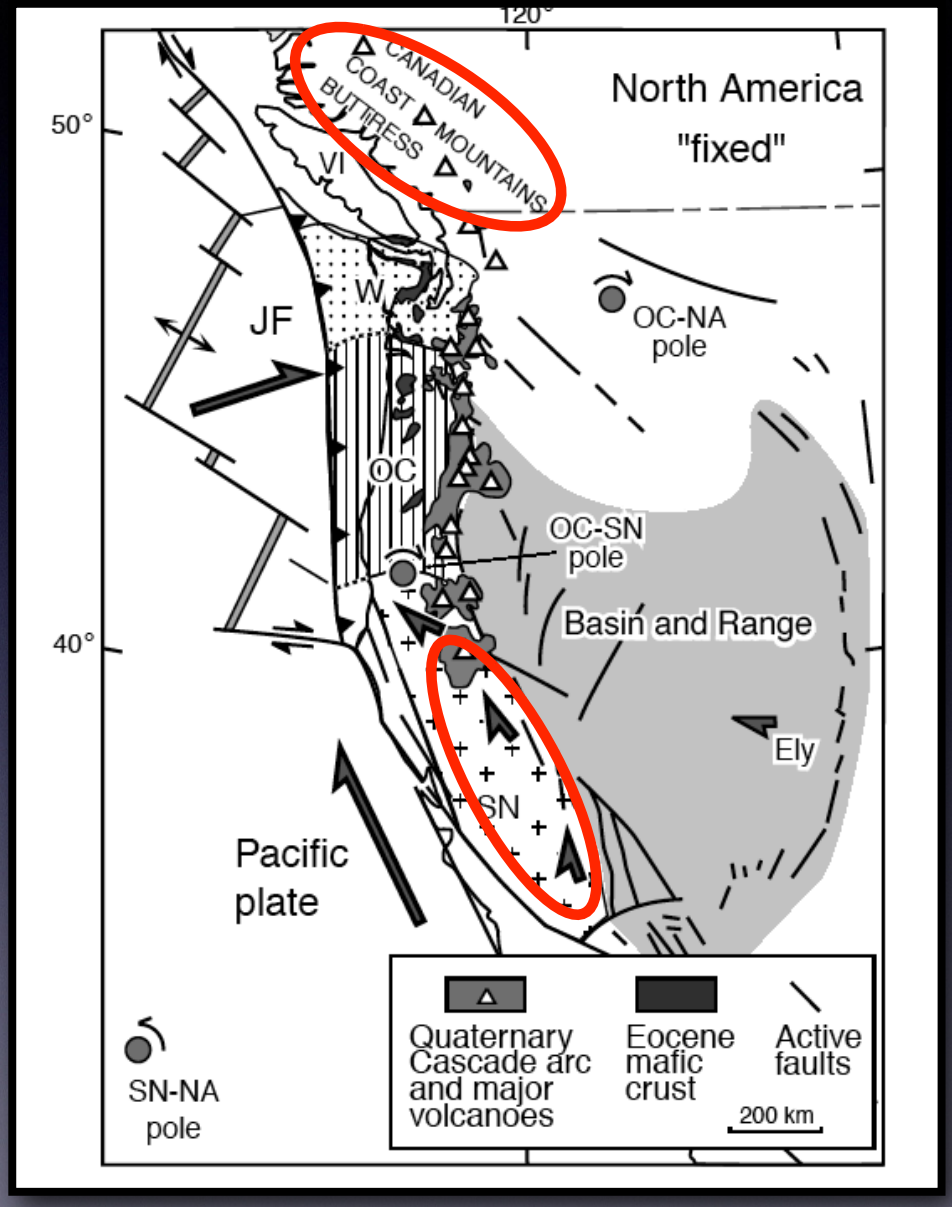

Figure 1. Tectonic setting of Cascadia. Juan de Fuca plate (JF) is subducting (barbed fault) beneath North America. Migrating Cascadia fore-arc terrane divided into Washington (W), Oregon Coastal (OC), and Sierra Nevada blocks (SN). "Instantaneous" Euler rotation poles shown for SN relative to North America (NA), OC-SN, and OC-NA. VI—Vancouver Island. (Modified from Argus and Gordon, 1991; Pezzopane and Weldon, 1993; Walcott, 1993.)

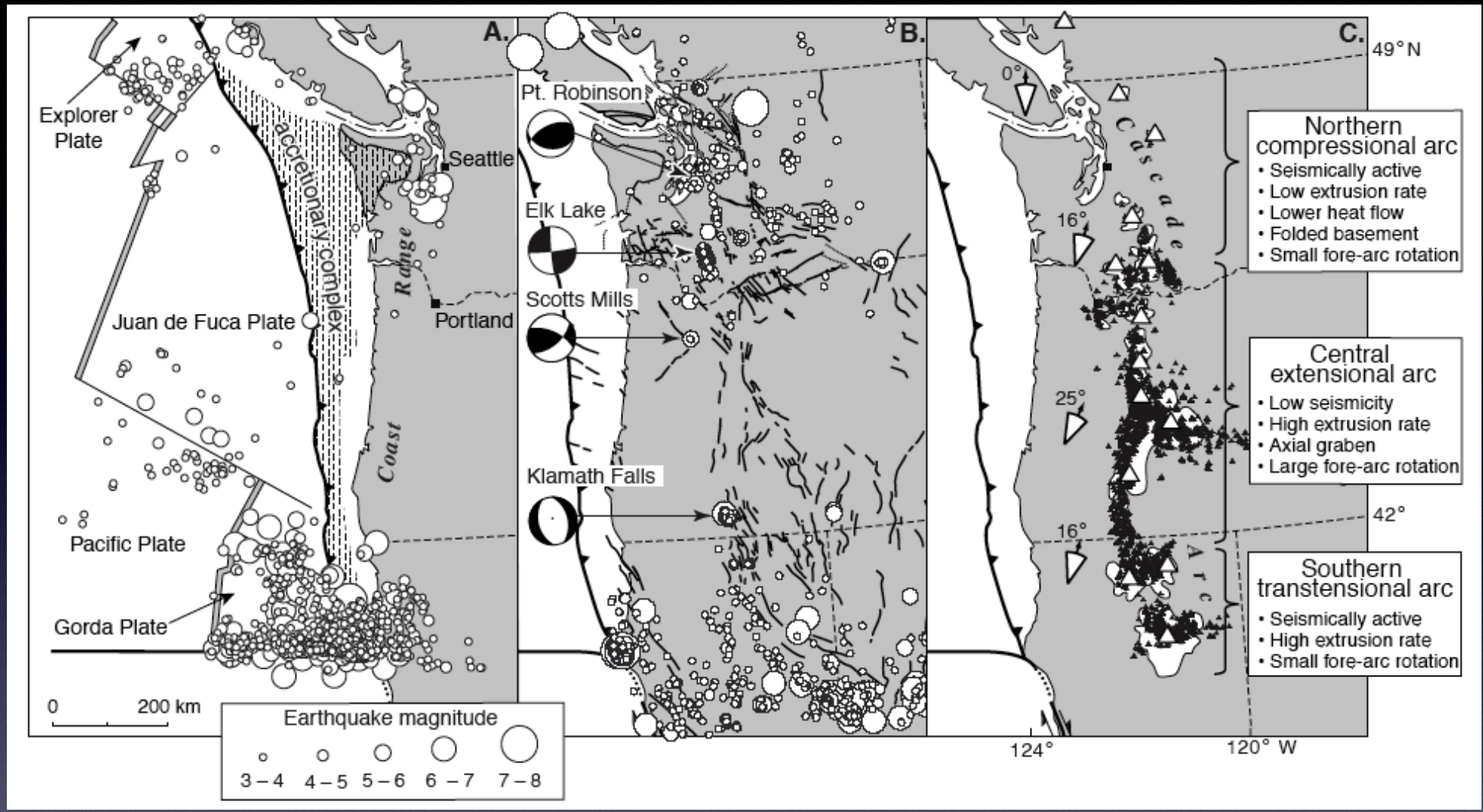

Lower Plate Seismicity

Upper Plate Seismicity

Arc Volcanism

Figure 2. Cascadia earthquakes, faults, volcanoes, and fore-arc rotation. A: Lower plate seismicity. B: Upper plate seismicity, recent focal mechanisms ($M_w > 5$), and late Cenozoic faults. C: Quaternary arc volcanism—white; major volcanoes—open triangles; post–5 Ma volcanic vents—filled triangles; fore-arc rotations with uncertainties—arrows (Pezzopane and Weldon, 1993; Sherrod and Smith, 1990; Guffanti and Weaver, 1988; Wells, 1990; Wiley et al., 1993; Madin et al., 1993).

Much of the Oregon forearc is comprised of the Siletzia terrain, ~35 km thick oceanic plateau. This is a strong crustal block.

Note the lack of uplift near Siletzia

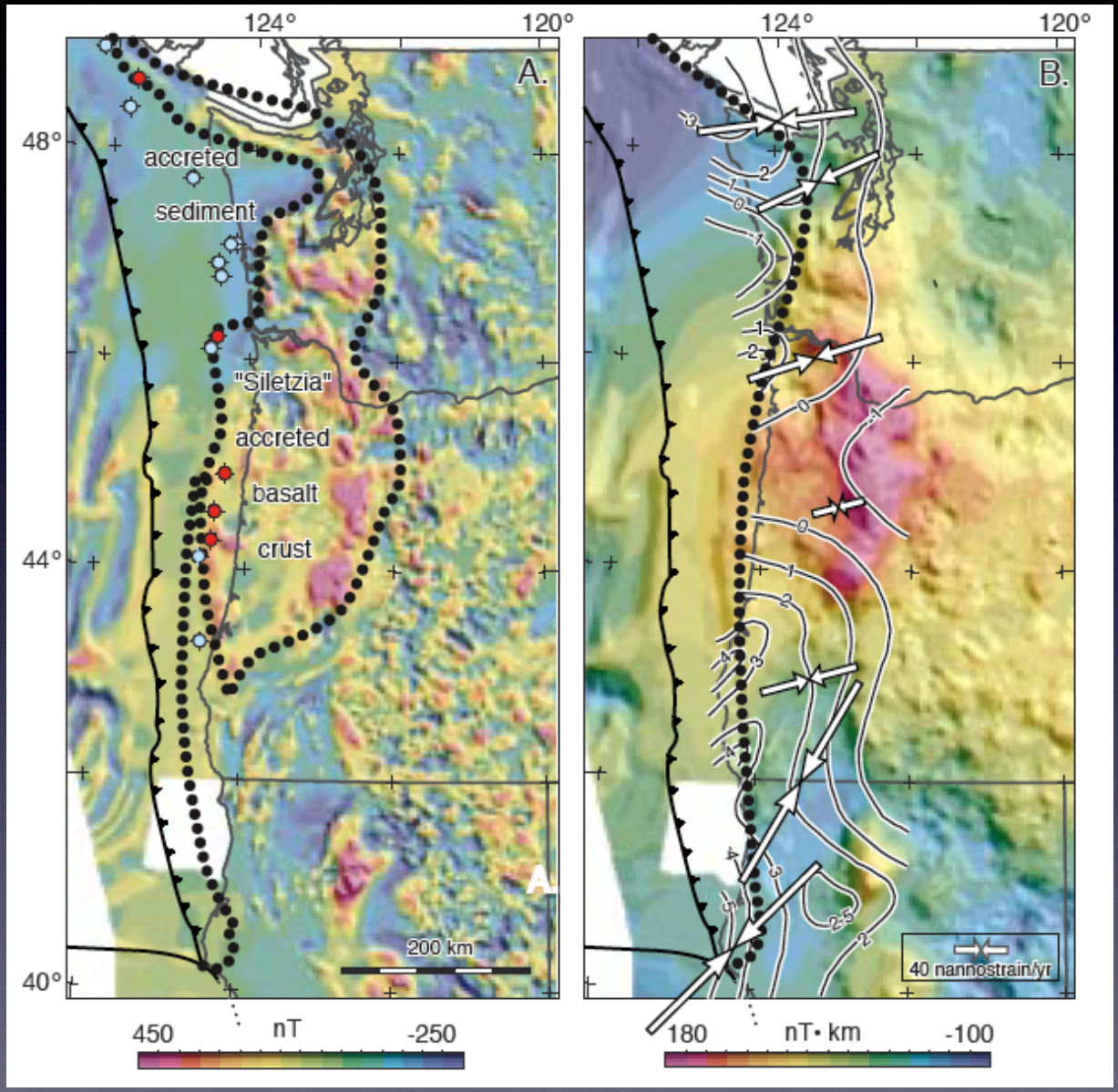

Figure 3. Magnetic and pseudogravity anomalies in the Cascadia fore arc. A: Siletzia, accreted basalt basement shown by magnetic high and offshore wells (filled circles) bottoming in basalt basement (red) and sediment (blue). Accreted sediments (magnetic low) outboard of Siletzia extend south to Mendocino triple junction. B: Pseudogravity anomaly (gravity that would be observed if magnetization were replaced by mass in 1:1 proportion) reflects total volume of Siletzia and coincides with low current uplift and margin contraction (contours in mm/yr, Mitchell et al., 1994; Murray and Lisowski, 1994, and 1998, written commun.) representing elastic strain accumulation above the locked subduction zone. Eastward limit of coupling (dotted) from Hyndman and Wang (1995).

- SNB moves NW, kicks out OC (Siletzia), compresses Washington against Canadian 'buttress'.
- Numbers are mm/yr
- Dextral slip and compression increase northward

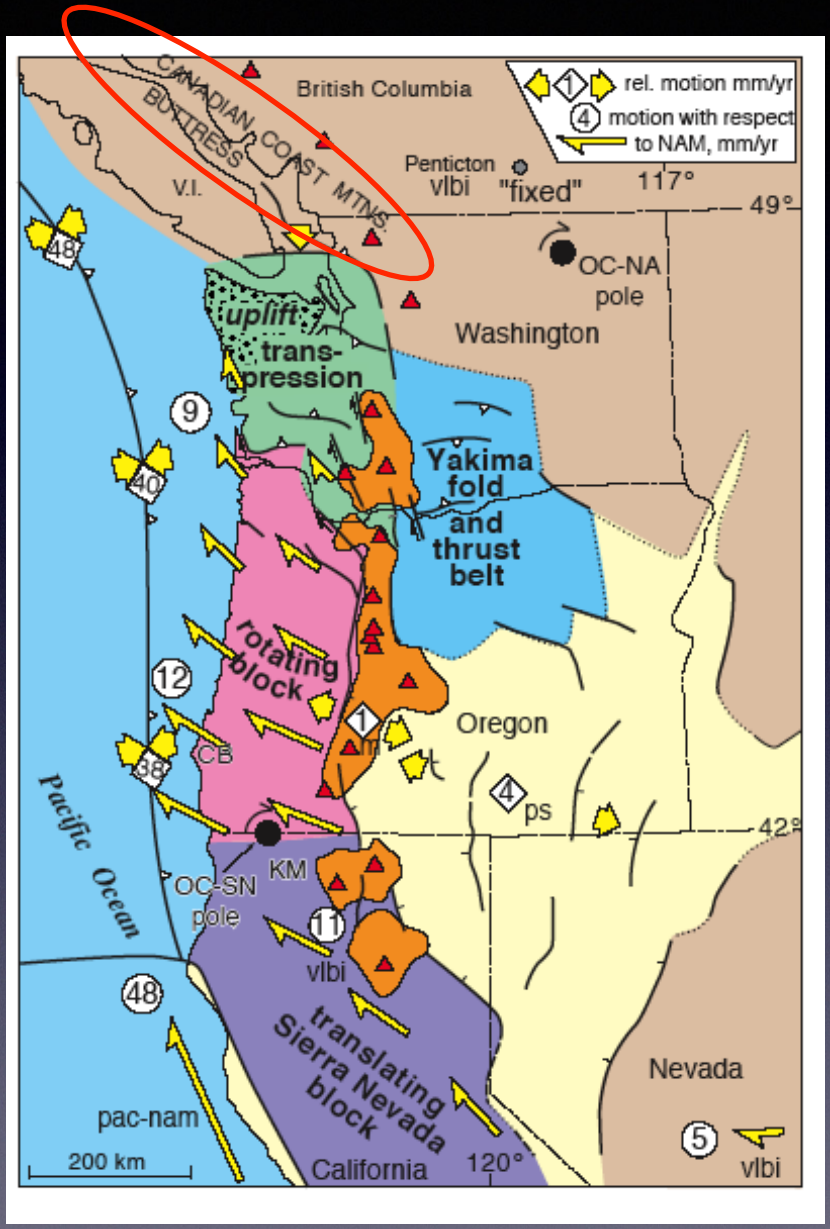

Figure 4. Velocity field for Cascadia fore arc calculated from OC-NA pole. Oregon block (pink) rotating at Neogene paleomagnetic rate is linked to Sierra Nevada block moving at vlbi rate by Euler pole (OC-SN) in Klamath Mountains (KM). Extensional arc forms along trailing edge of Oregon fore-arc block which absorbs Sierra Nevada displacement by rotating over trench at Cape Blanco (CB). North end of Oregon block deforms Washington fore arc (green) against Canadian buttress, causing north-south compression, uplift, thrust faulting, and earthquakes. Rates from very long baseline interferometry (vlbi); paleoseismology (ps); magmatic spreading (m); Pacific–North America motion (pac-nam); other symbols as in Figure 1.

Figure 5.6-5: Crustal deformations associated with the India-Eurasia palte collision.

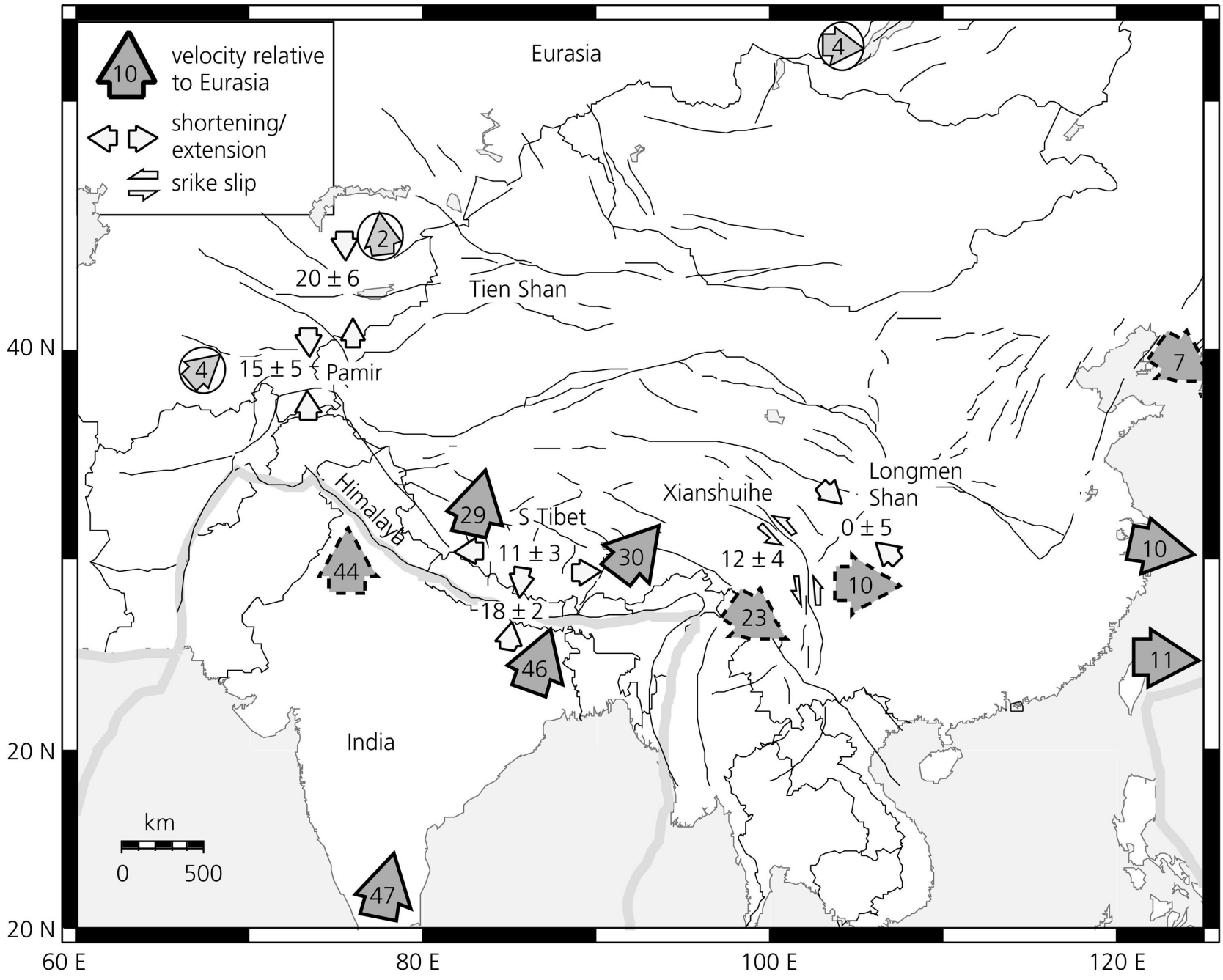

Figure 5.6-7: Plasticine model for the deformation of Asia as a result of the collision with India.

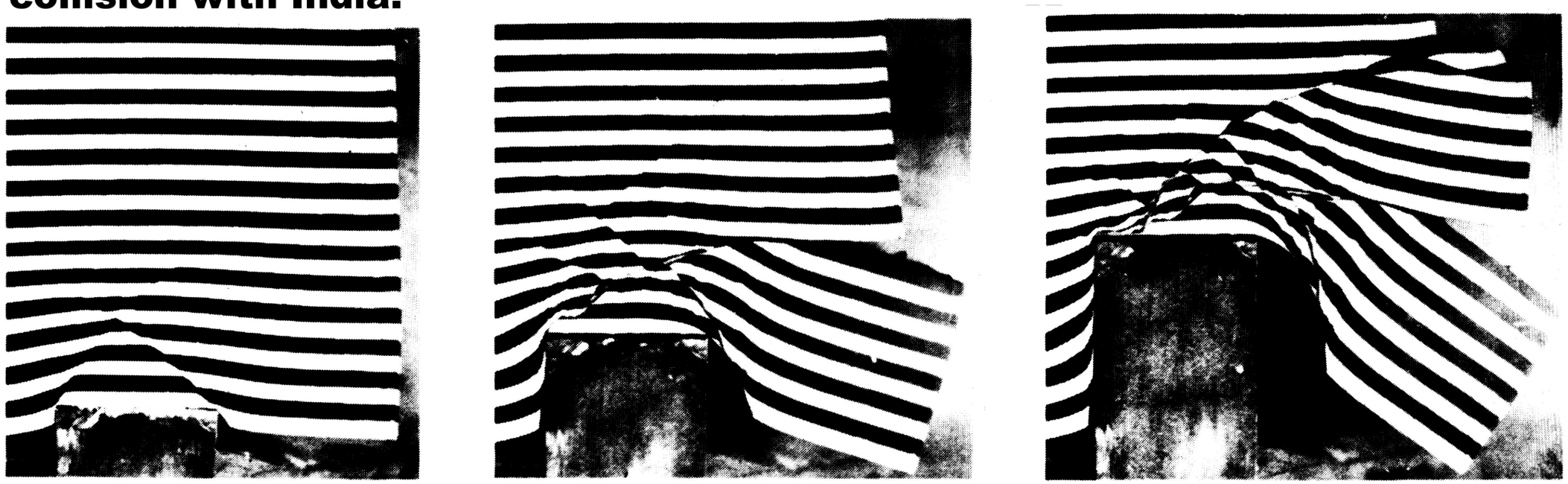

Early analog model of Tibetan Tectonics:
Extrusion of (semi) rigid blocks

Figure 5.6-6: Focal mechanisms are Himalayan continental convergence zone.

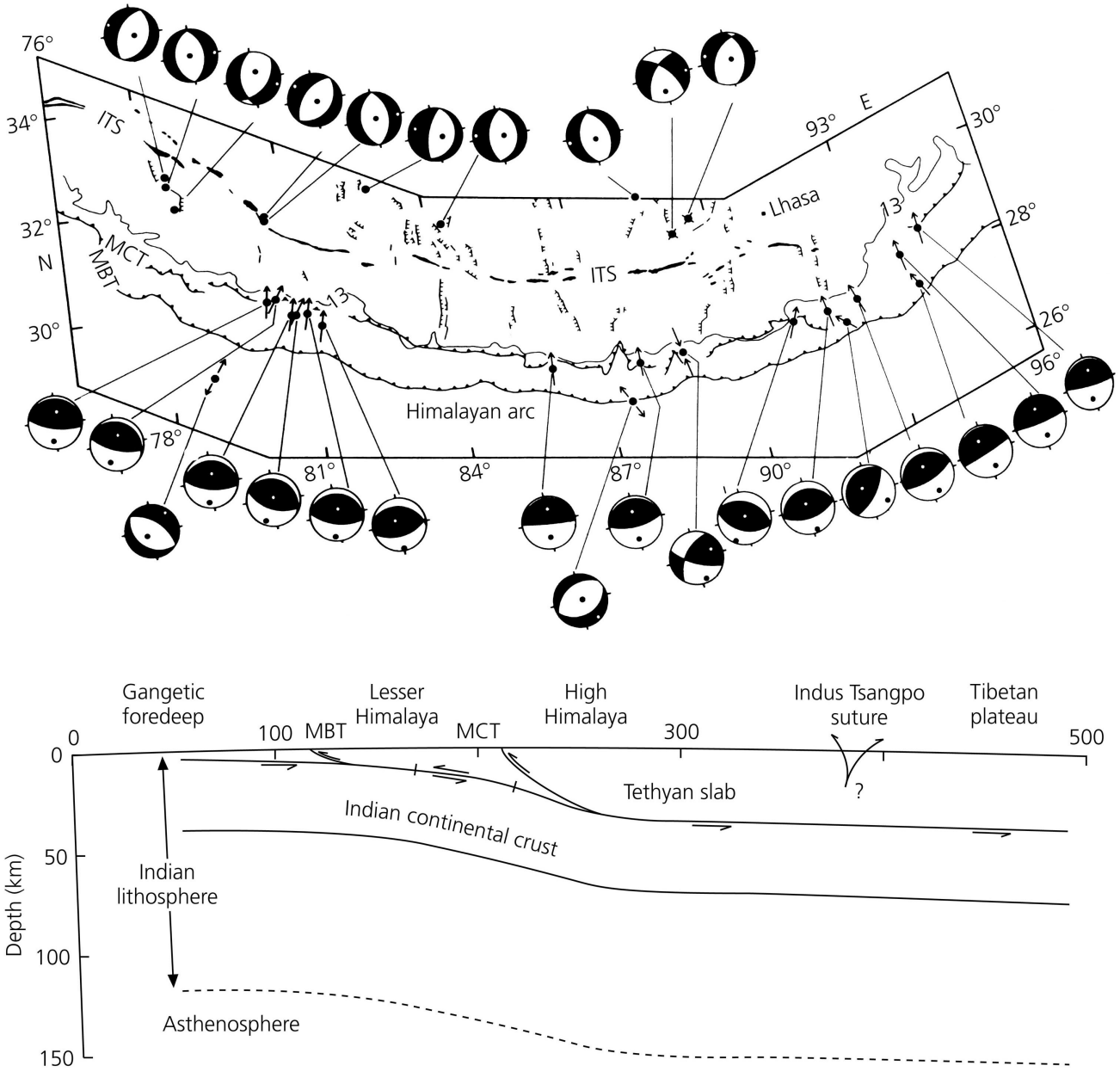

JOURNAL OF GEOPHYSICAL RESEARCH, VOL. 112, B01401, doi:10.1029/2005JB004244, 2007

Click Here for Full Article

Microplate model for the present-day deformation of Tibet

Wayne Thatcher[1]

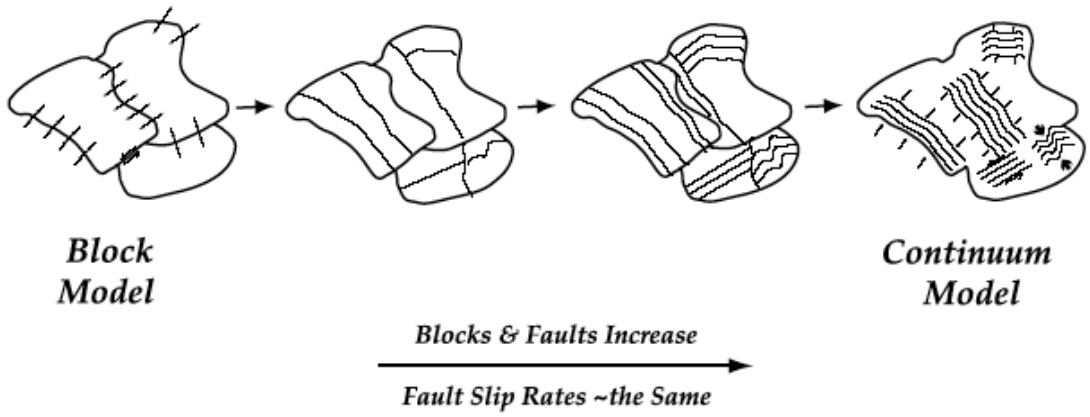

Figure 1. Schematic cartoon of end-member kinematic models for continental deformation with possible transitions from one to the other.

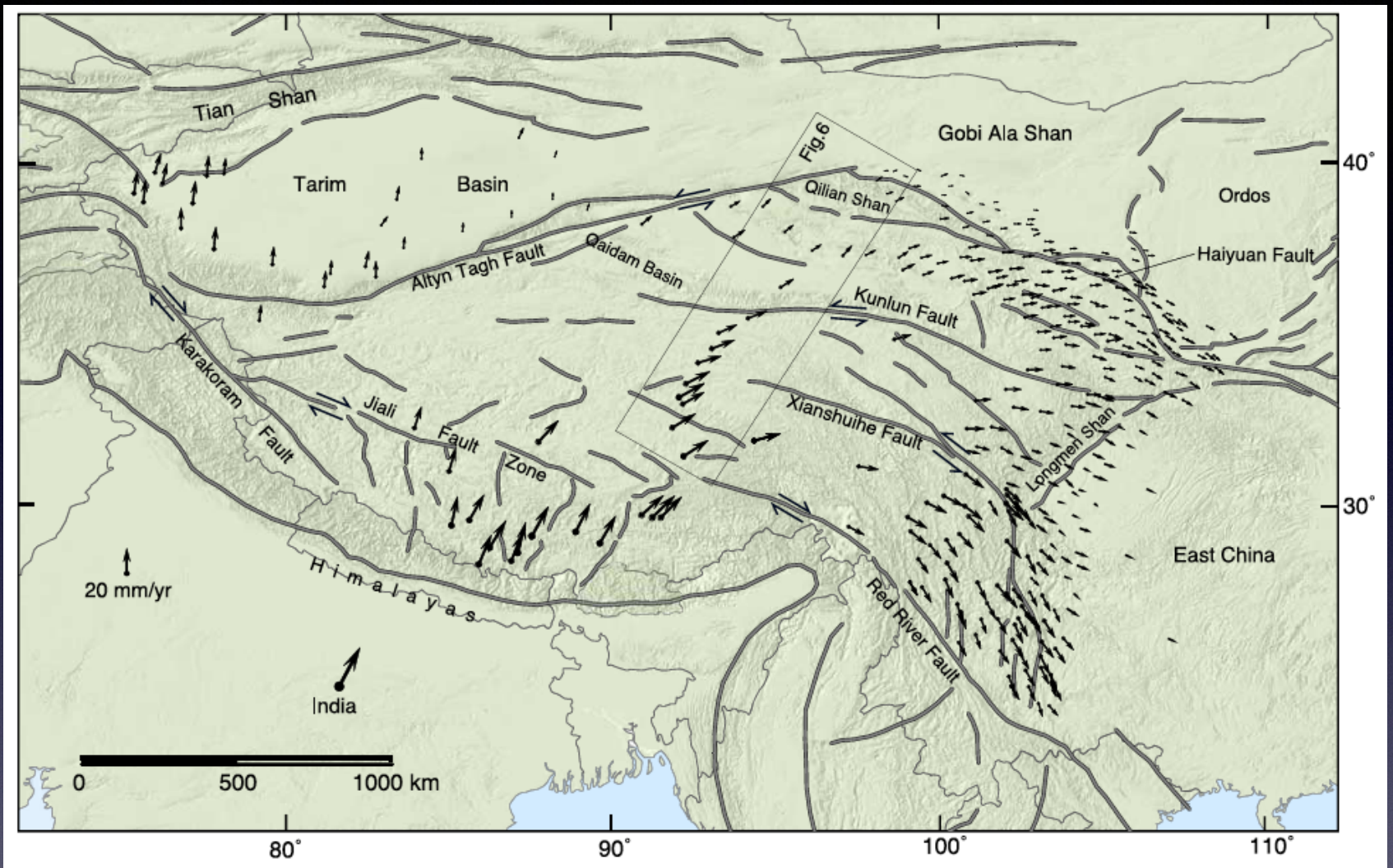

Figure 2. Tibet and surrounding regions, with GPS velocity vectors relative to stable Eurasia (to the north of map area). Velocity uncertainties are generally 1–2 mm/yr, so most error ellipses are illegible at this scale and are not plotted. Gray lines show active faults. Paired arrows show sense of slip on major strike-slip faults (except, to avoid clutter, for the Haiyuan fault, which is left lateral). Major faults and regions discussed in the text are labeled for reference. Rectangle shows location of profile for which observed and model-predicted velocities are plotted in Figure 6.

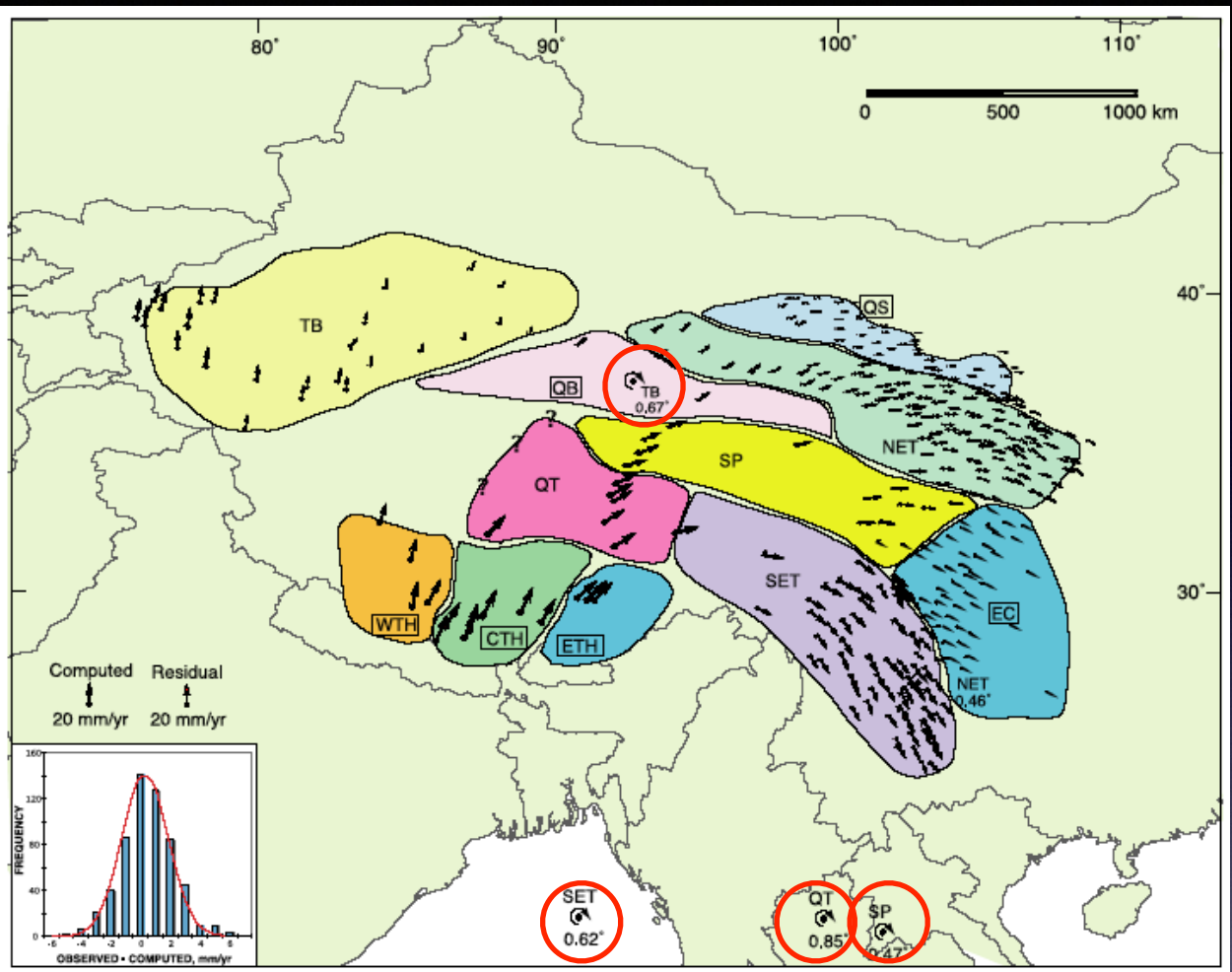

Figure 3. Observed velocity field (black arrows) and block model of Tibet. Blocks are color coded with abbreviated names as indicated. Smaller arrows show differences between observed and computed velocities (many are too small to be seen at true scale; these residuals are shown alone at an expanded scale in Figure 4). Inset shows histogram of residuals, which are fit well by a Gaussian distribution with mean of 0.4 and standard deviation of 1.6 mm/yr. Euler poles (rotation axes) and rotation rates (in degrees per million years) are shown for five blocks (NET, northeast Tibet; QT, Qiangtang; SET, southeast Tibet; SP, Songpan; TB, Tarim Basin). Average translation velocities relative to Eurasia are shown for six additional blocks whose abbreviated names are enclosed by rectangles (CTH, central Tibet Himalaya; EC, east China; ETH, eastern Tibet Himalaya; WTH, western Tibet Himalaya; QB, Qaidam Basin; QS, Qilian Shan). Block model parameters along with data and model fit statistics are listed in Tables 1 and 2.

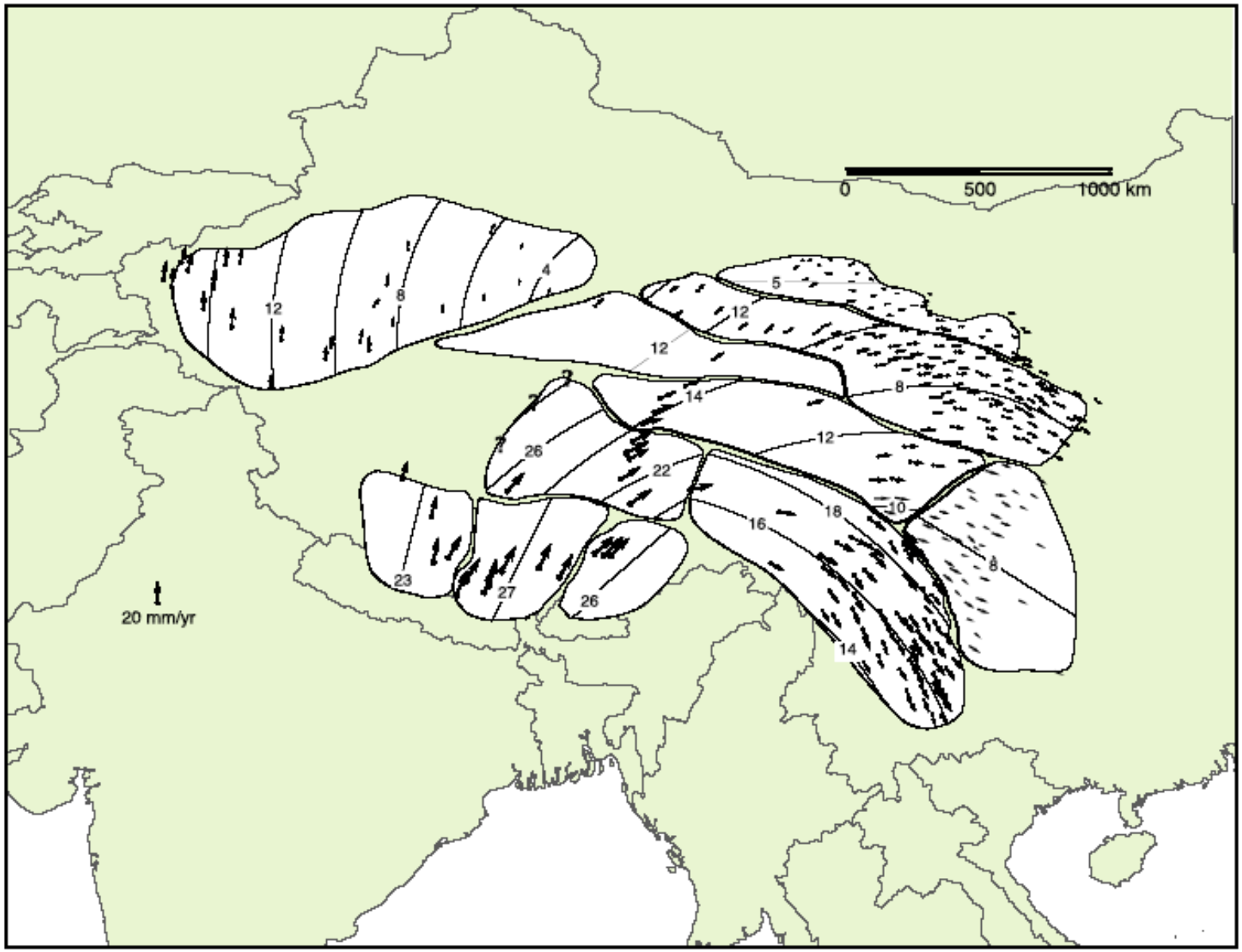

Figure 5. Observed GPS velocities, outlines of blocks used to fit observations, and predicted block motions (faint lines and arcs, with predicted velocities in mm/yr).

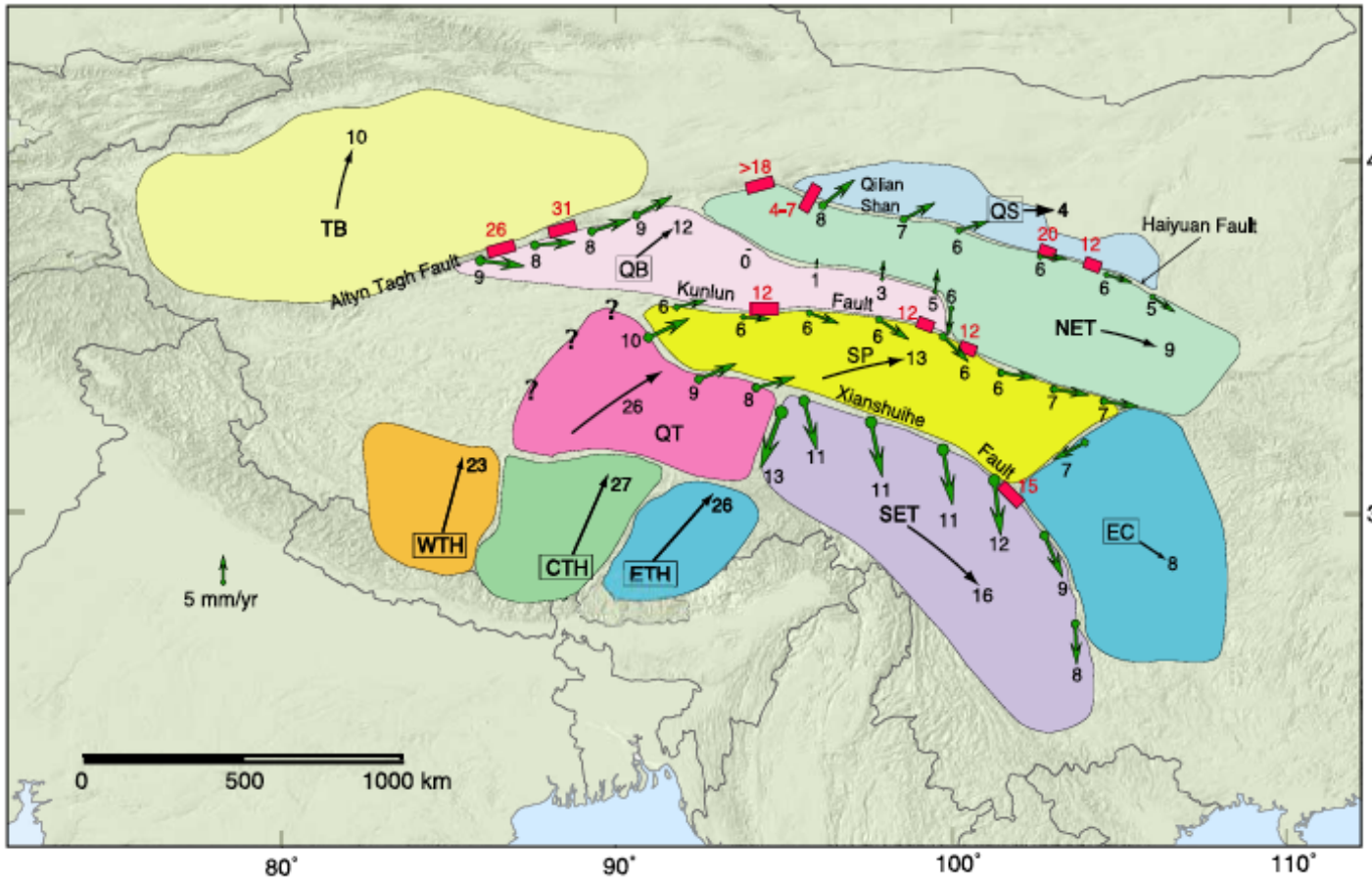

Figure 7. Predicted interblock velocities (thicker green arrows with numbers), with average block velocities relative to Eurasia (thinner black arrows) and geologically estimated slip rates (red numerals). All rates are in mm/yr. Blocks are color coded with names abbreviated as in Figure 3. The convention on interblock vectors is to show the motion of the southern block relative to its northern neighbor, or the eastern block relative to its western mate. Typical rates of motion (relative to Eurasia) near the centers of five rotating blocks are shown by arcs drawn from each of their Euler poles, with arc length proportional to velocity and arrowheads indicating the sense of rotation. The abbreviated names of five additional rigidly translating blocks are enclosed by faint rectangles. Their translation velocities relative to Eurasia are shown as thin straight arrows. Red rectangles show locations of sites where geological estimates of fault slip rate have been obtained by radiometric dating [*Ryerson et al.*, 2006; *Allen et al.*, 1991]; red numerals give the late Pleistocene-Holocene slip rates.

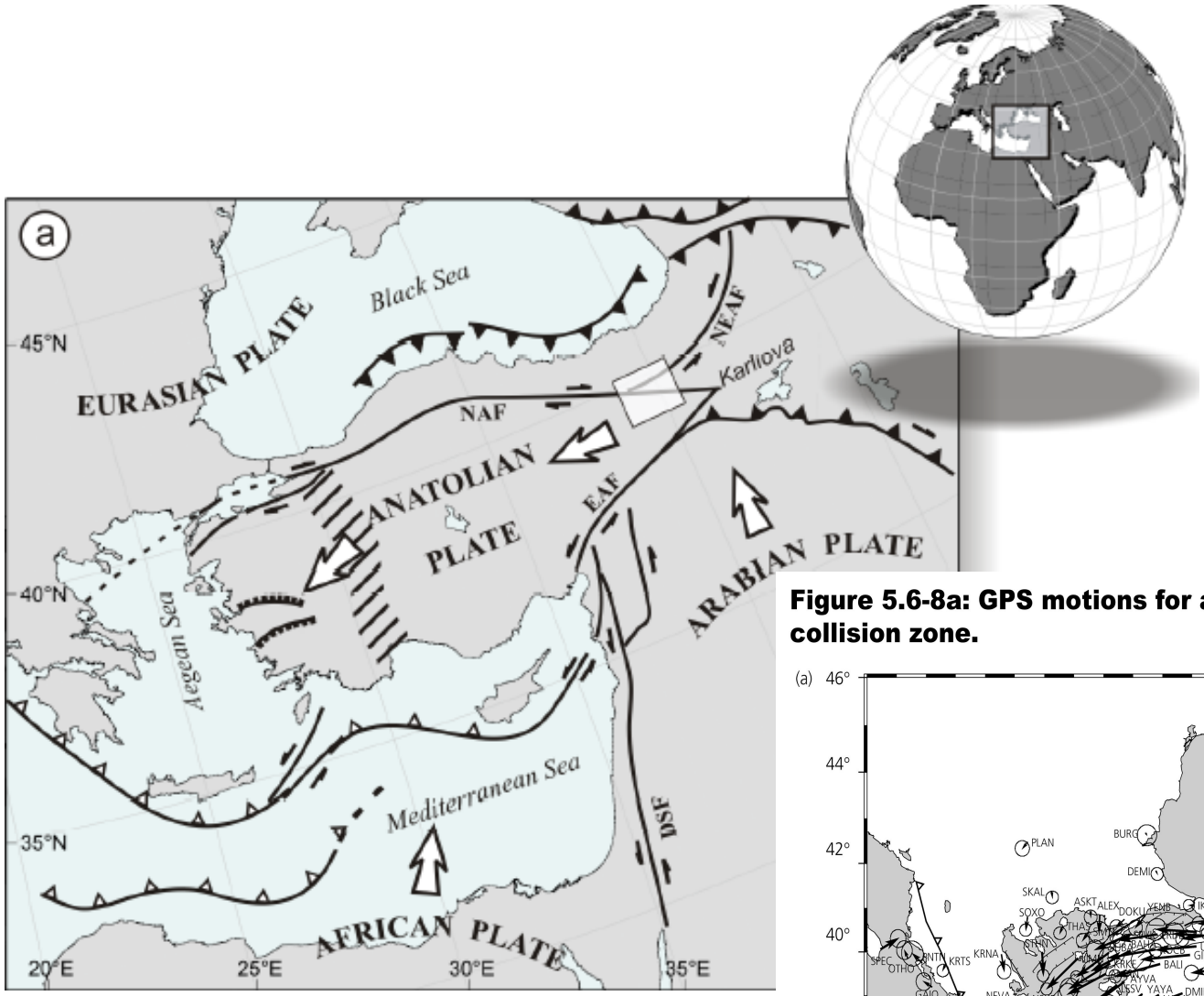

Figure 5.6-8a: GPS motions for a portion of the Africa-Arabia-Eurasia plate collision zone.

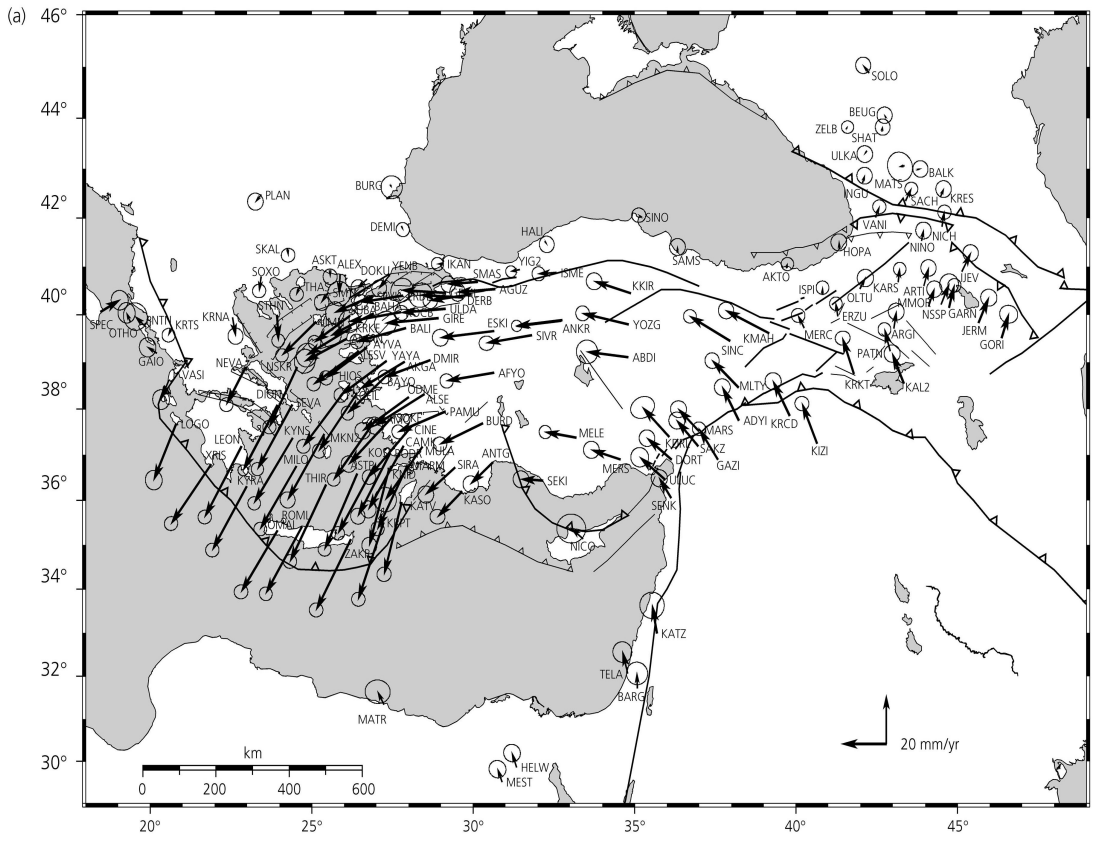

2nd Example of Extrusion Tectonics modeled as blocks

Figure 5.6-8b: Focal mechanisms for a portion of the Africa-Arabia-Eurasia plate collision zone.

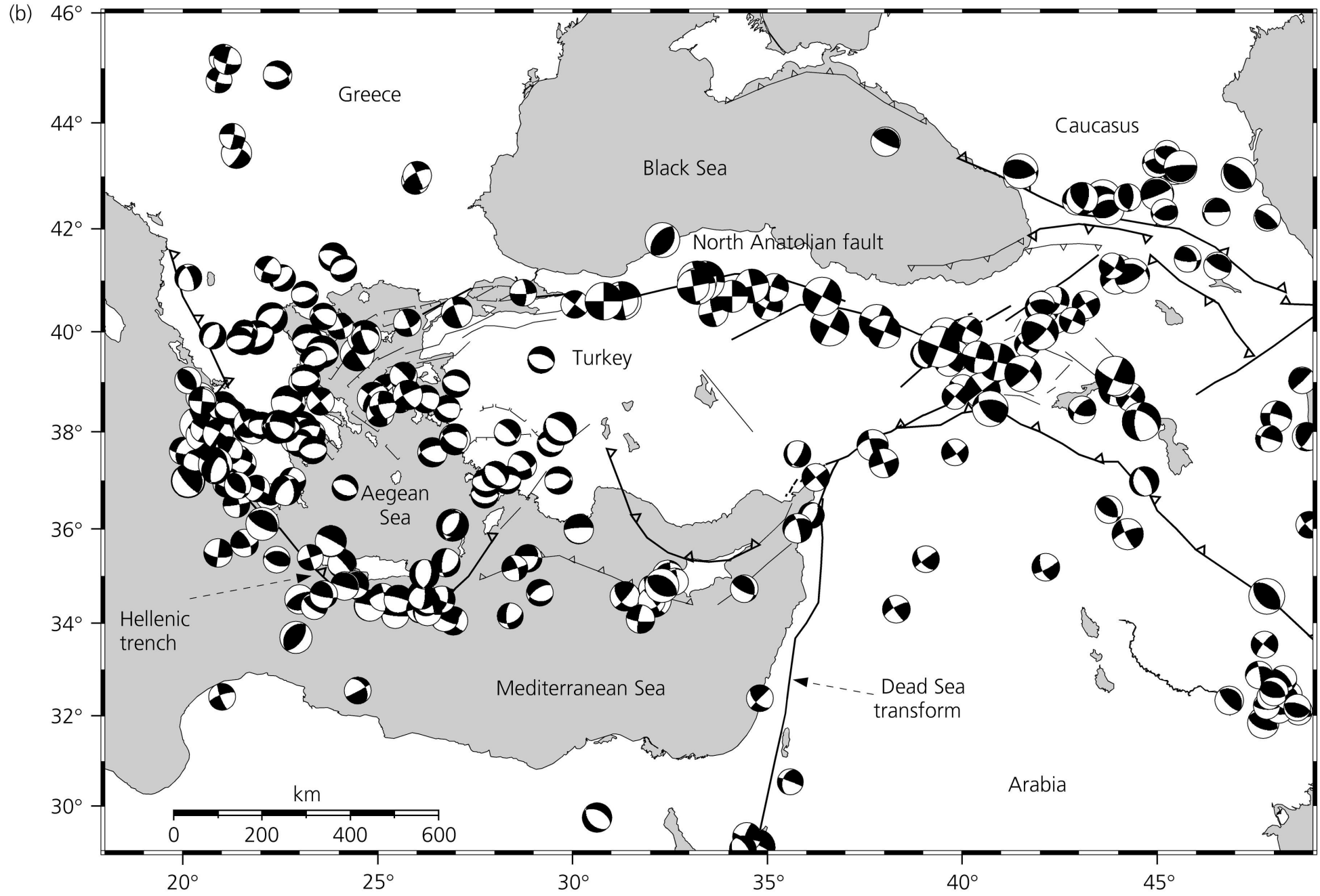

Figure 5.6-8c: Tectonic interpretation for a portion of the Africa-Arabia-Eurasia plate collision zone.

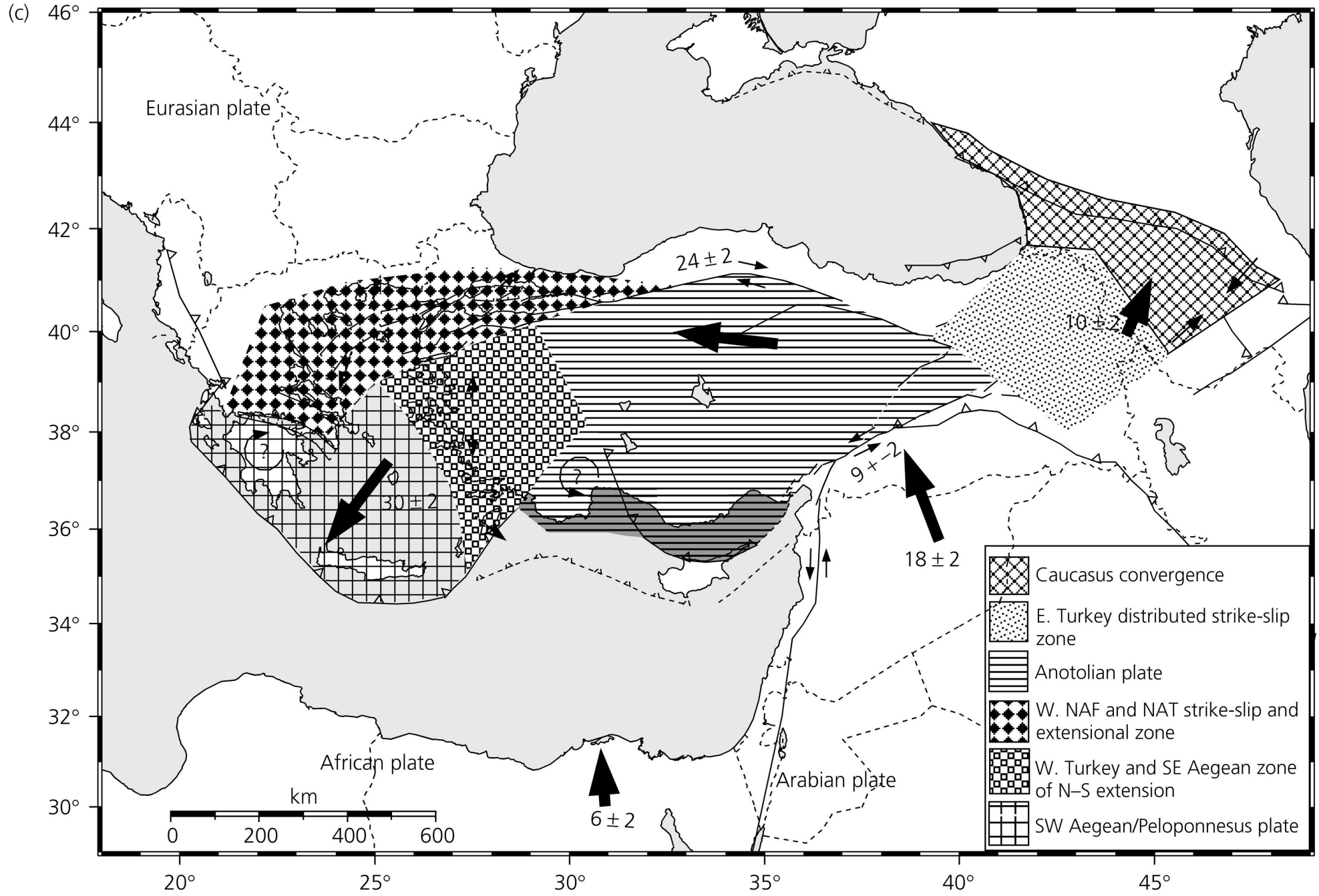

Jelly Sandwich vs. Creme Brulée

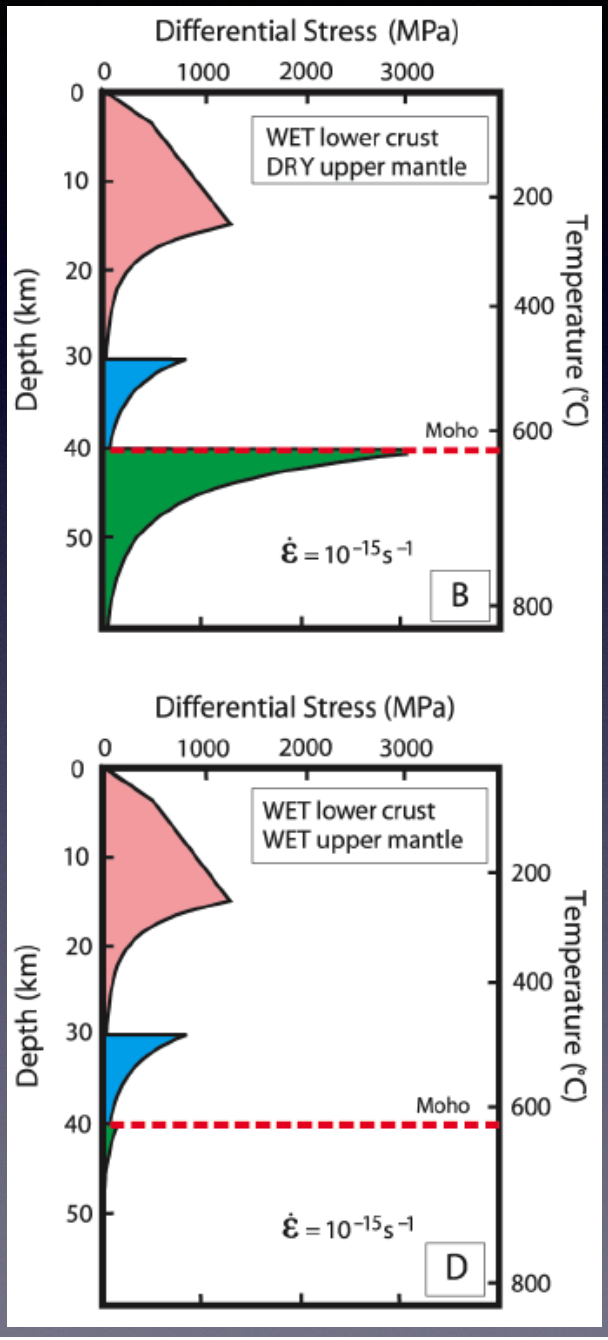

Long-standing view of strength profile for continents, motivated by Chen and Molnar (1983)

"If significant strength resides only in the seismogenic layer of the continental lithosphere, it would not be surprising if regional patterns of active faulting at the surface were dominated by the strength of the crustal blocks and the interactions between them. The strength of the faults themselves is then presumably a limiting factor in crustal behavior, but remains very uncertain (e.g., Scholz, 2000)." [Jackson, 2002]

Creme Brulée

Strength Curves

- How do rocks deform in the lithosphere?
  - mechanisms
- What are the load bearing parts of the lithosphere?
  - strength
- Must consider
  - Brittle crust
  - Ductile crust

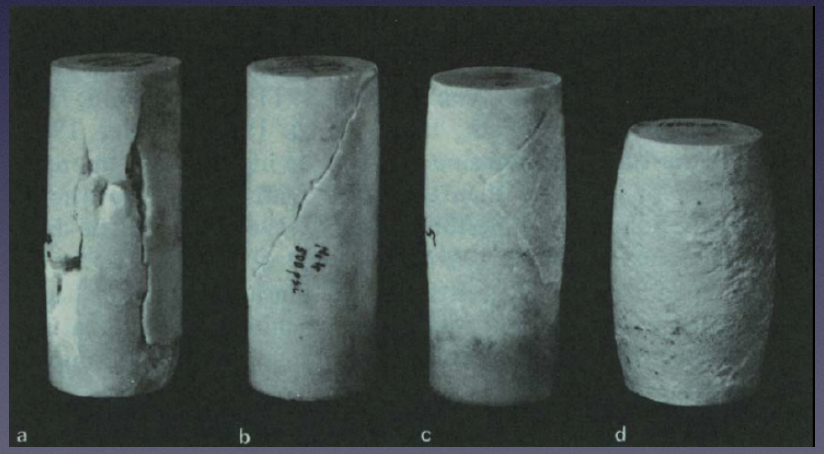

Figure 5.7-1: Elastic and plastic rheologies.

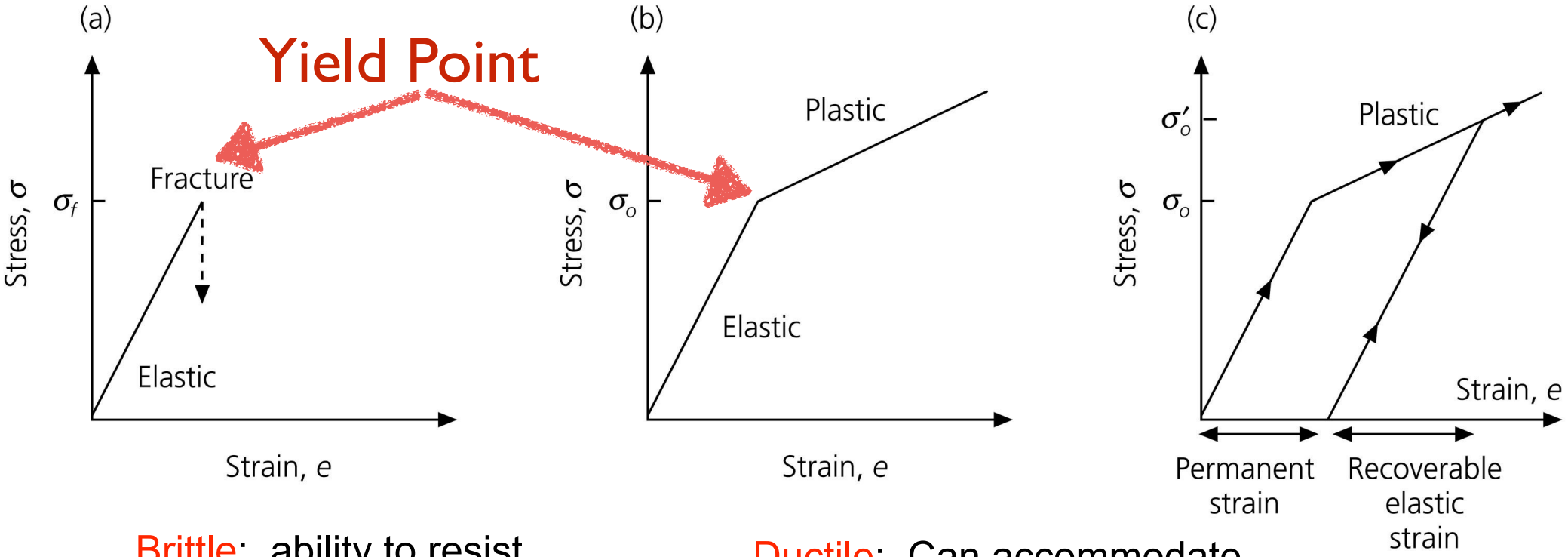

Brittle: ability to resist load decreases with permanent strain.

Fracture Stress

Ductile: Can accommodate permanent strain without losing its ability to resist load

Yield Stress

Deformation Depends On

	Elastic/Brittle	Ductile/Plastic
Composition	----------	
Temperature	low	high
Pressures	low	high
Rate	high	low
Grain Size	----------	

Linear	Linear or non-linear
$\sigma \propto \varepsilon$	$\partial\varepsilon/\partial t \propto \sigma$
$\sigma_{ij} \propto C_{ijkl}\varepsilon_{kl}$	$\partial\varepsilon/\partial t \propto \sigma^n$

Brittle-ductile transition

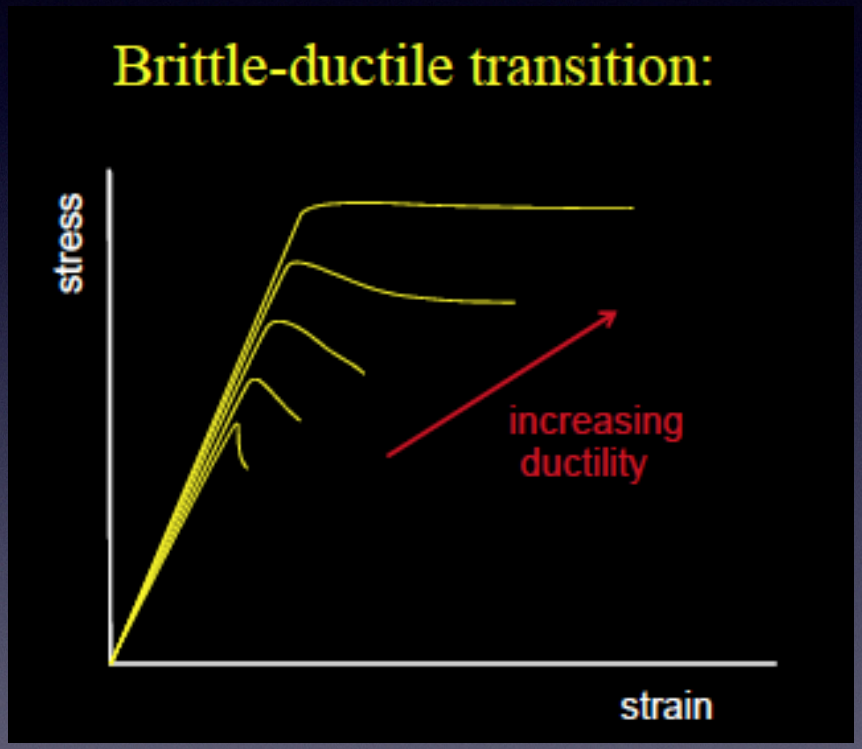

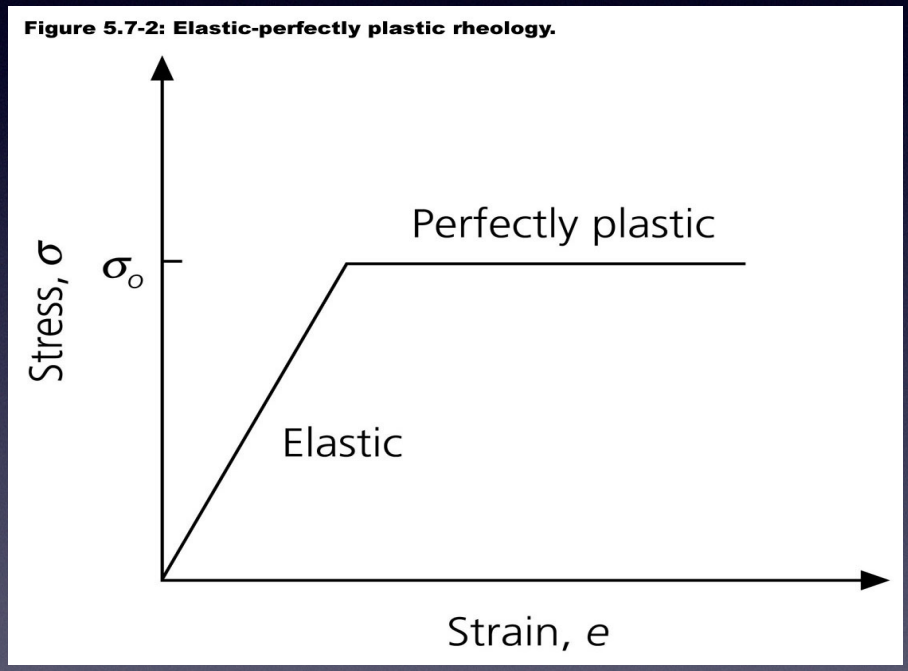

Mode of failure versus Mechanism

- Mode of failure
  - Stress-strain curve
  - Homogeneous spreading or deformation
    - distributed (ductile)
    - localized (brittle)
- Mechanism of failure
  - cataclastic
  - crystal plastic/diffusion

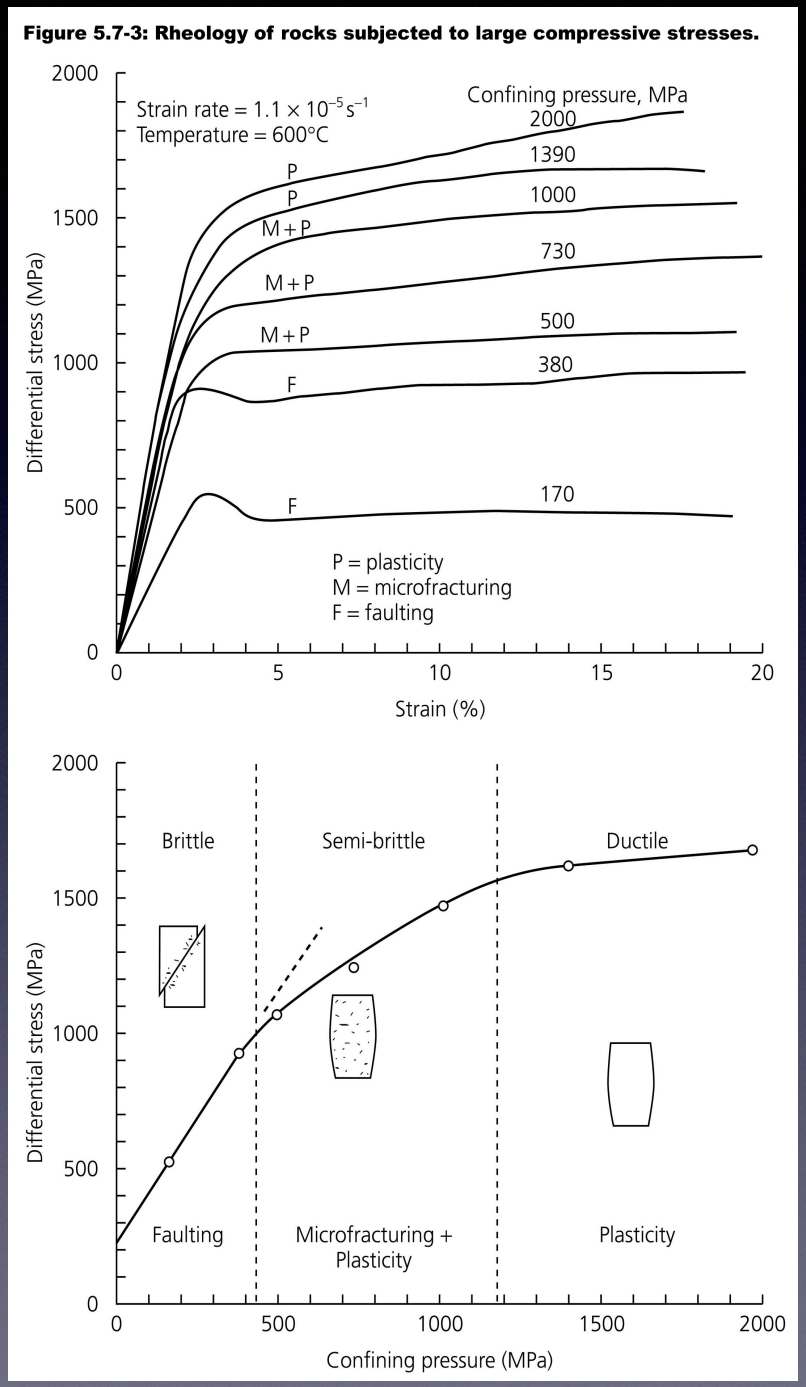

- Mode of Failure

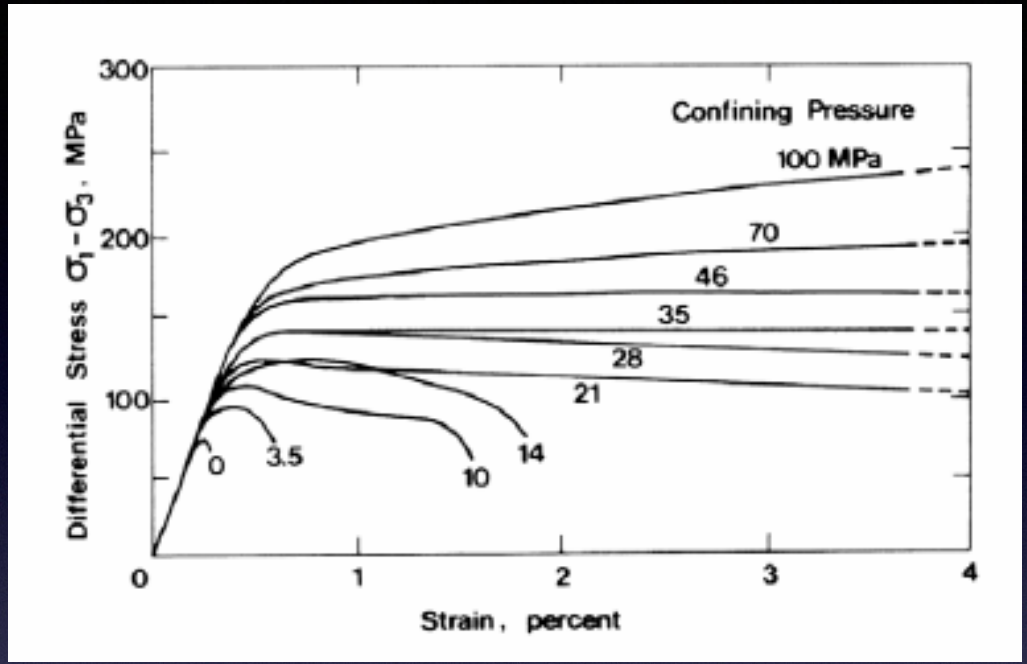

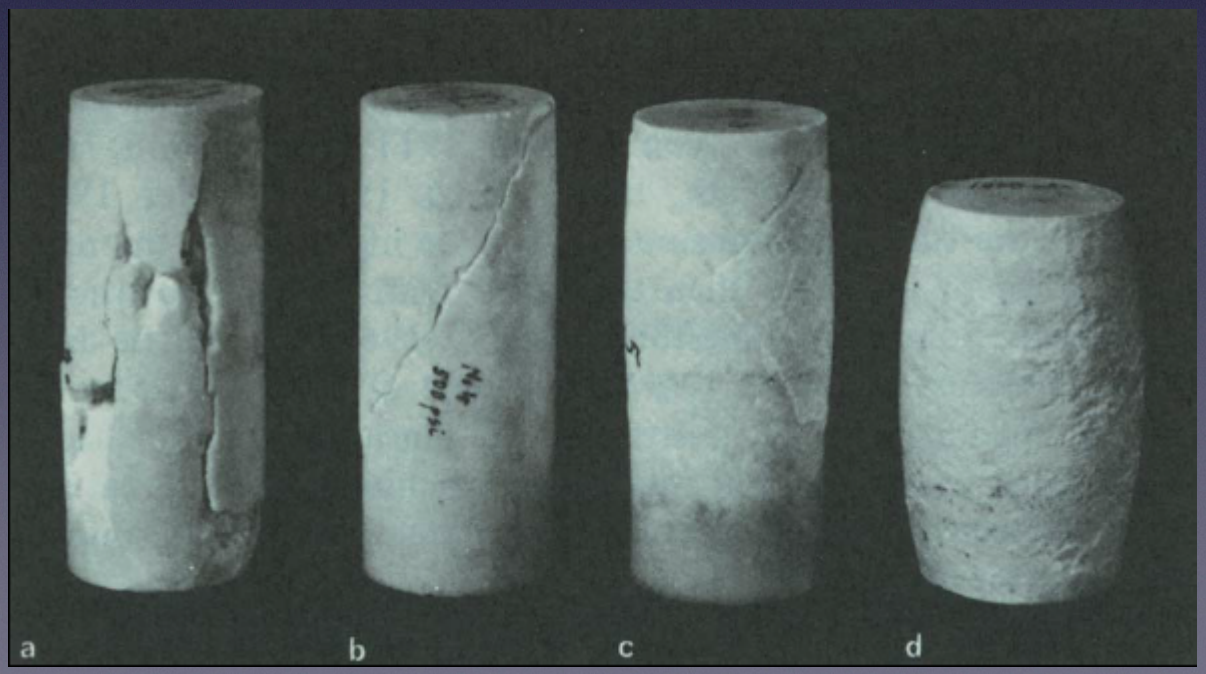

Brittle Failure
Shear Stress vs. Normal Stress

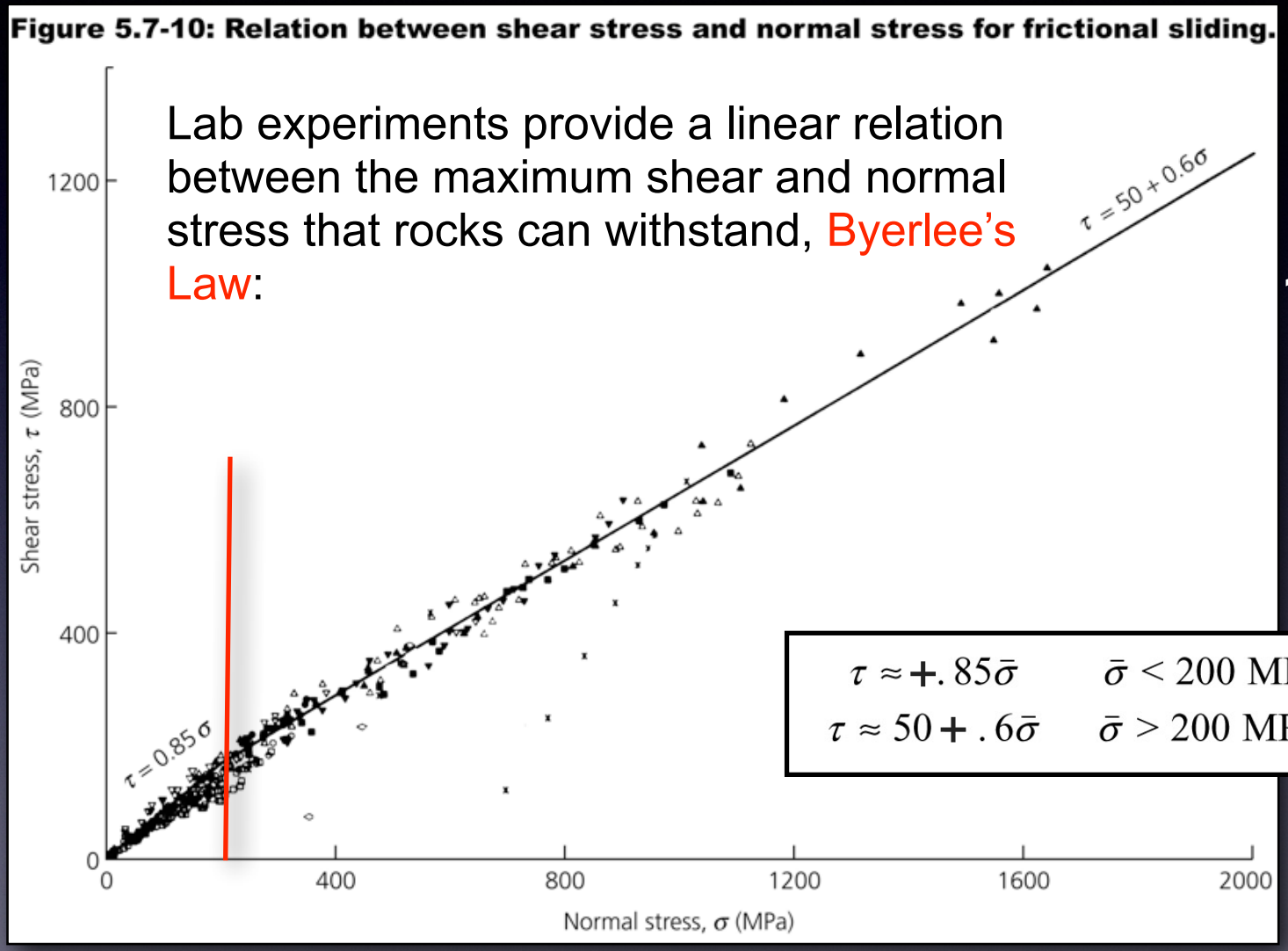

τ shear stress

σ normal stress

1 kbar = 100 MPa

1GPa ~ 30 km, 100MPa~3 km

Plastic Deformation

- Material behaves like a fluid, but still has elasticity; 'elastoviscious' behavior
- Deformation accomated by two mechanisms:
  - Intracrystalline plasticity
  - Diffusive mass transfer

General form of flow law

$$\dot{\varepsilon} = A(\sigma_1 - \sigma_3)^n e^{\left(\frac{-H}{RT}\right)}$$

- ε = strain rate, s-1
- n = stress exponent
- H = activatin enthalpy, J mol^-1
- R = gas constant, J K-1 mol-1
- T = temperature, K

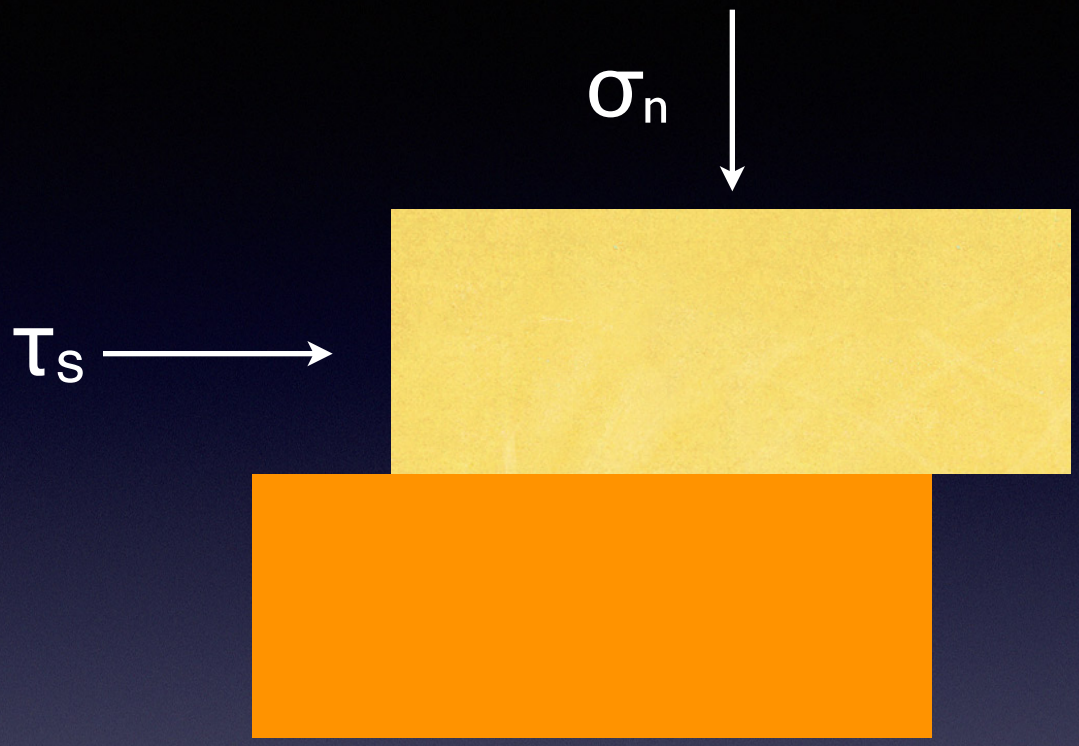

$$\tau_s = \mu_f \sigma_n + C_f$$

Cohesive Strength

Coefficient of friction

Byerlee's law for frictional slideing, also Mohr-Columb failure criteria

Failure criteria plotted on resolved shear vs. normal stress

$\mu_f \sim 0.6$ to 0.8 for Nearly all rocks!

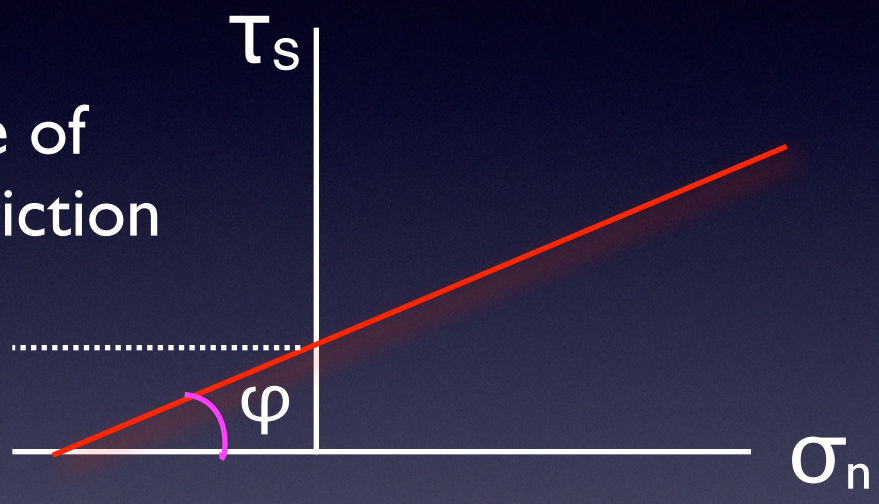

φ, angle of internal friction

In absence of normal stress, cohesive strength is the minimum shear stress required to cause failure

$\tau_s = \mu_f \sigma_n + C_f$

Cohesive Strength

Coefficient of friction

Byerlee's law for frictional slideing, also Mohr-Columb failure criteria

$\tau_s = \sigma_n \tan \varphi + C_f$

How can we know when failure occurs in a particular stress condition?

- Given Byerlee's law for brittle failure, how can we know if the stress conditions within the crust will result in permanent deformation?
- Mohr's Circle: gives stress on planes of arbitrary orientation, combine this with Byerlee's law
  - Derive by force balance (bb)
  - Derive by coordinate rotation of stress tensor

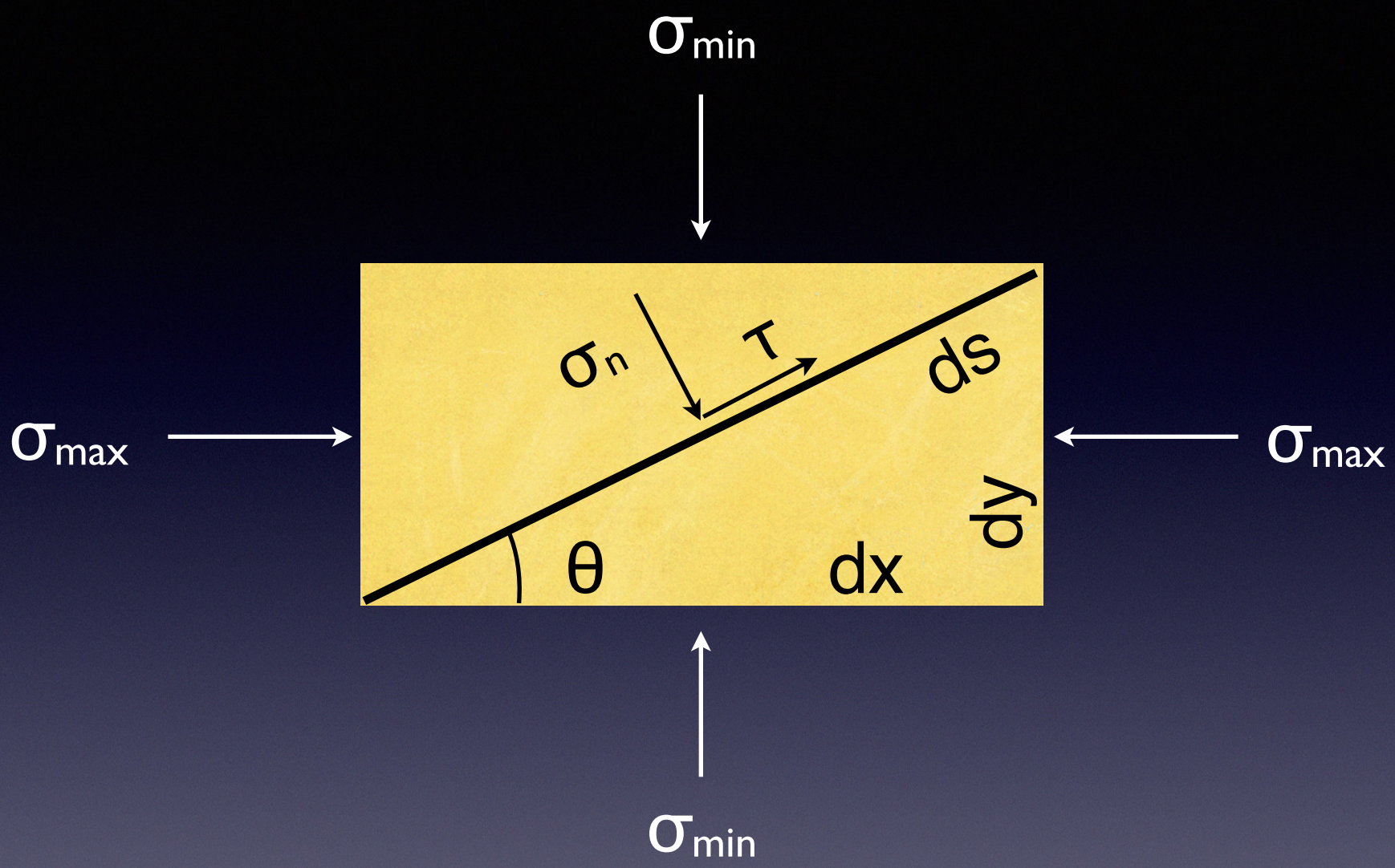

Derivation of Mohr's Circle: Resolve principal stresses into a plane of arbitrary orientation. Balance forces in the σ_n and τ directions

Normal and shear stresses can be expressed as:

$\sigma_n = \sigma_c + \sigma_r \cos 2\theta$

$\tau = \sigma_r \sin 2\theta$

Equations of a circle with center at σ_c and a radius of σ_r

$\sigma_c = (\sigma_1 + \sigma_3)/2$

$\sigma_r = (\sigma_1 - \sigma_3)/2$

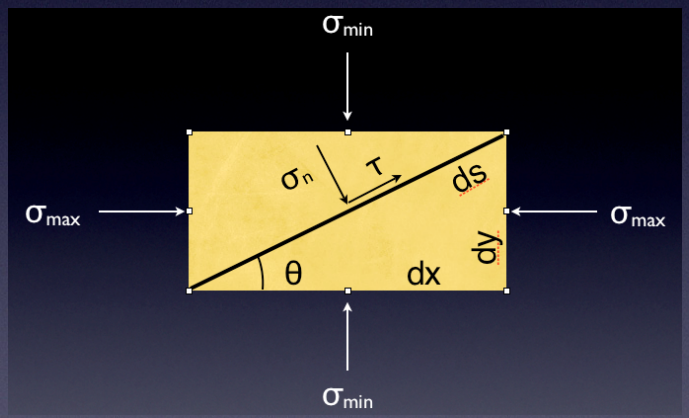

$\tau_s = \sigma_n \tan \varphi + C_f$

$\theta = \varphi/2 + \pi/4$

φ, angle of internal friction

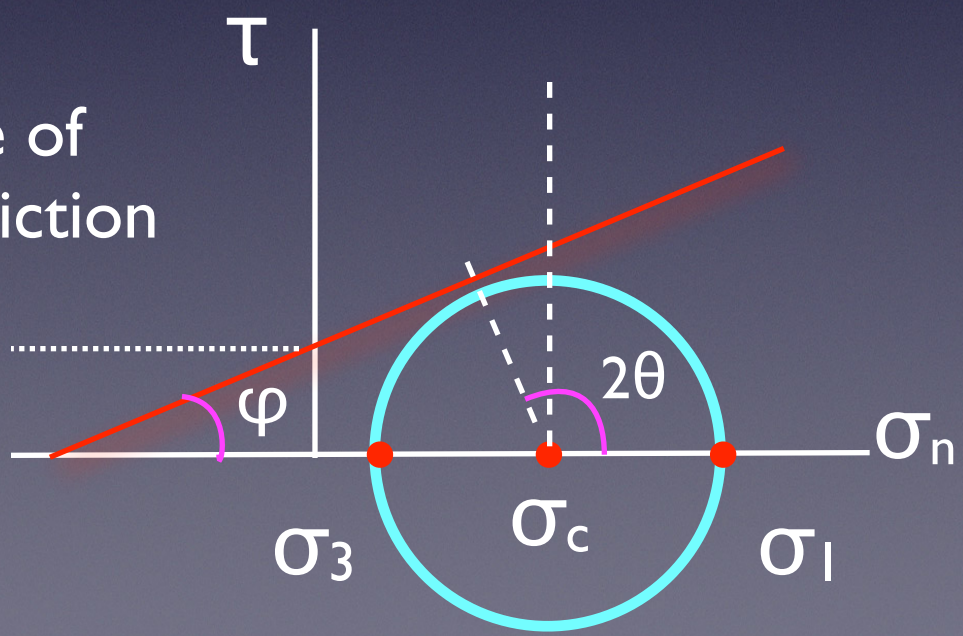

Figure 5.7-8: Failure with and without internal friction.

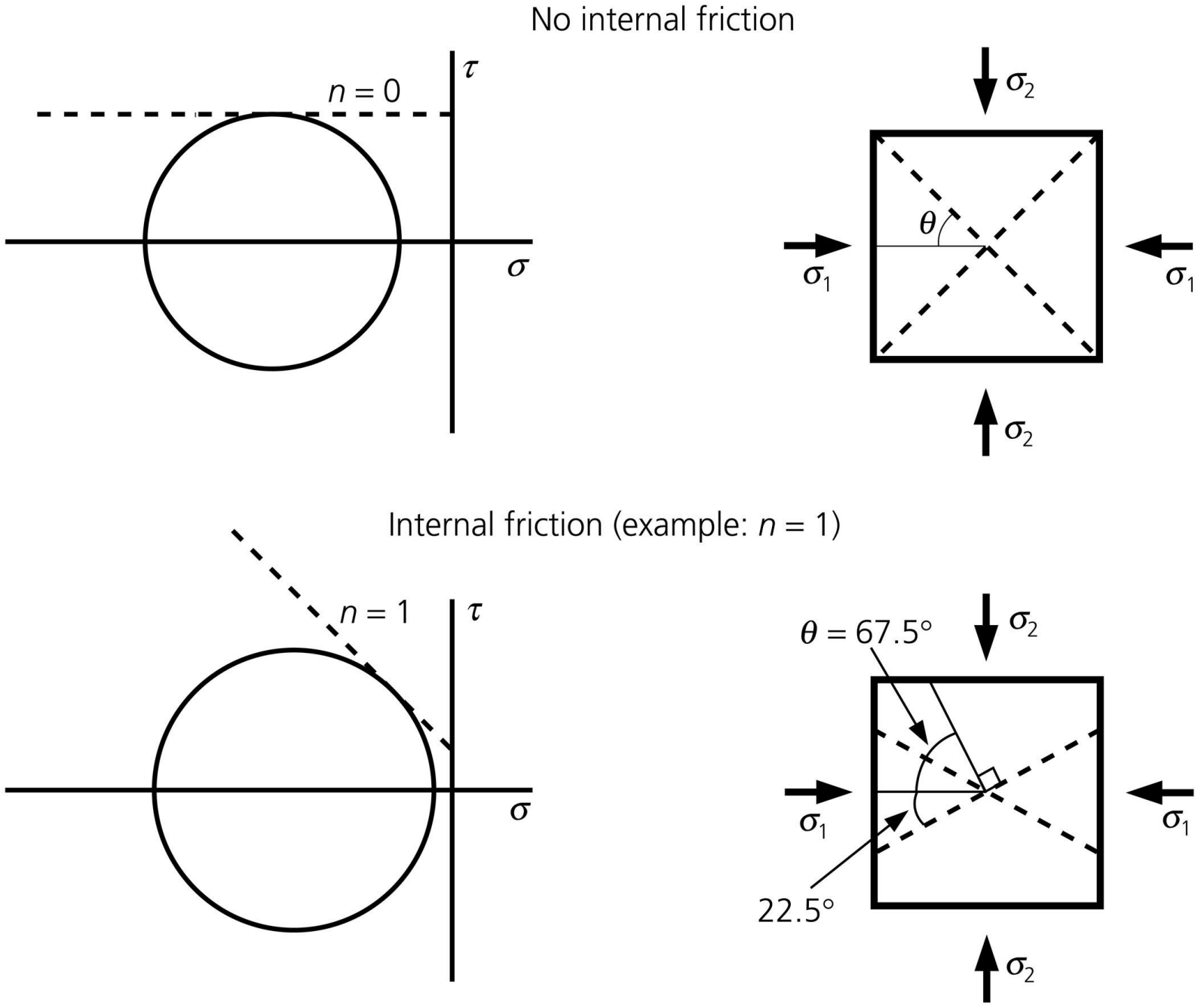

Mohr's Circle via coordinate rotation of stress tensor

If the coordinate axes ($\hat{\mathbf{e}}_1$, $\hat{\mathbf{e}}_2$) are oriented in the principal stress directions, the stress tensor is diagonal,

$$\sigma_{ij} = \begin{pmatrix} \sigma_1 & 0 \\ 0 & \sigma_2 \end{pmatrix}$$

Now rotate the coordinate system by an angle θ: $\quad A = \begin{pmatrix} \cos\theta & \sin\theta \\ -\sin\theta & \cos\theta \end{pmatrix}$

$$\sigma'_{ij} = A\sigma A^T = \begin{pmatrix} \cos\theta & \sin\theta \\ -\sin\theta & \cos\theta \end{pmatrix}\begin{pmatrix} \sigma_1 & 0 \\ 0 & \sigma_2 \end{pmatrix}\begin{pmatrix} \cos\theta & -\sin\theta \\ \sin\theta & \cos\theta \end{pmatrix} = \begin{pmatrix} \sigma_1\cos^2\theta + \sigma_2\sin^2\theta & (\sigma_2 - \sigma_1)\sin\theta\cos\theta \\ (\sigma_2 - \sigma_1)\sin\theta\cos\theta & \sigma_1\sin^2\theta + \sigma_2\cos^2\theta \end{pmatrix}$$

Figure 5.7-4: Normal and shear stresses as a function of geometry.

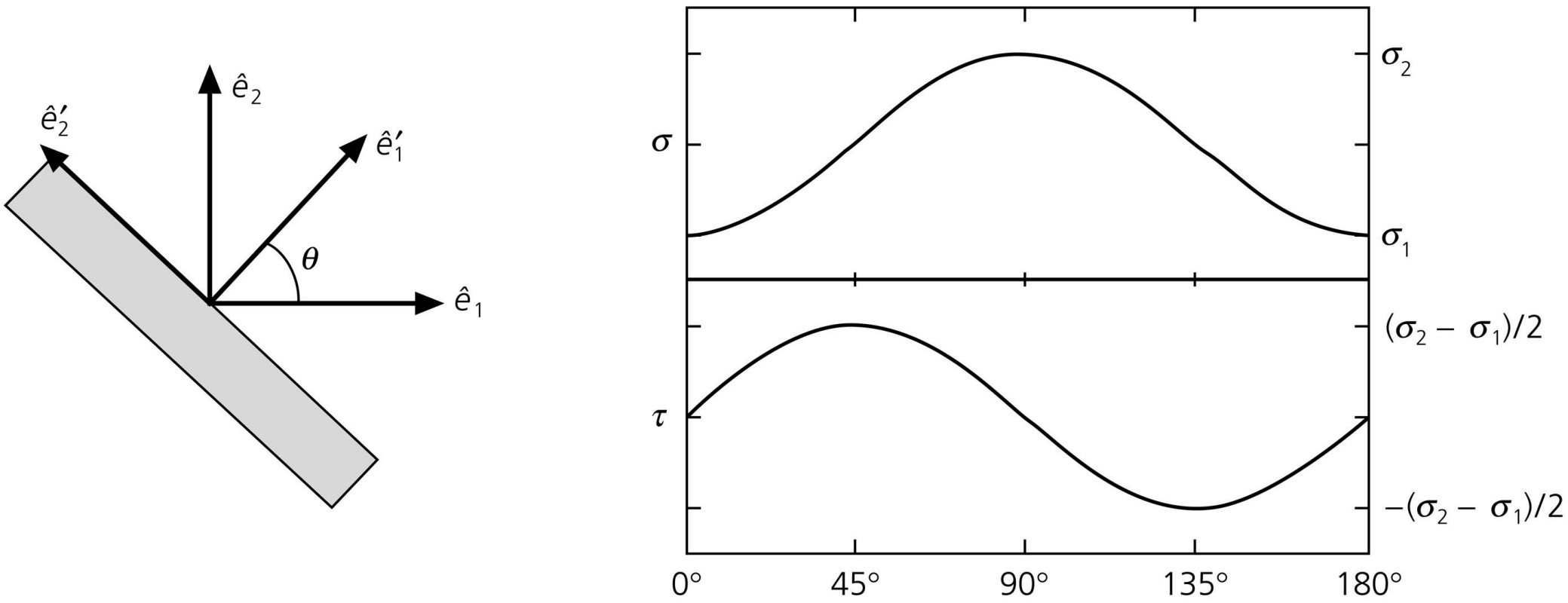

Normal stress:

$$\sigma = \sigma'_{11} = \sigma_1 \cos^2\theta + \sigma_2 \sin^2\theta = \frac{(\sigma_1 + \sigma_2)}{2} + \frac{(\sigma_1 - \sigma_2)}{2}\cos 2\theta$$

Shear stress:

$$\tau = \sigma'_{12} = (\sigma_2 - \sigma_1)\sin\theta\cos\theta = \frac{(\sigma_2 - \sigma_1)}{2}\sin 2\theta.$$

Mohr's circle shows the values of σ and τ as functions of θ (the angle between the normal to a plane and the principal stress direction, σ_1.

Figure 5.7-5: Definition of Mohr's circle.

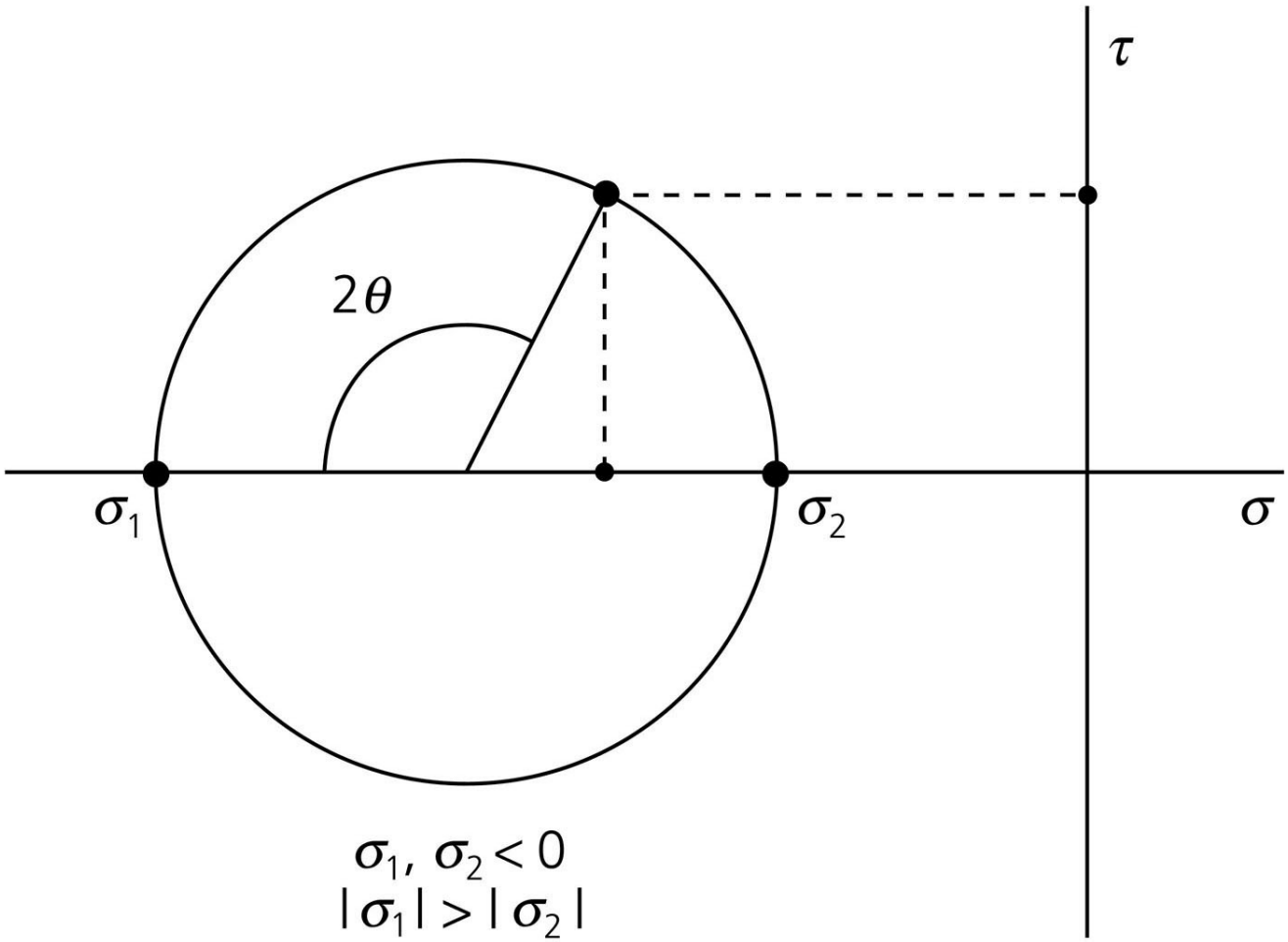

Normal stress:

$$\sigma = \sigma'_{11} = \sigma_1 \cos^2\theta + \sigma_2 \sin^2\theta = \frac{(\sigma_1 + \sigma_2)}{2} + \frac{(\sigma_1 - \sigma_2)}{2}\cos 2\theta$$

Shear stress:

$$\tau = \sigma'_{12} = (\sigma_2 - \sigma_1)\sin\theta\cos\theta = \frac{(\sigma_2 - \sigma_1)}{2}\sin 2\theta.$$

Mohr's circle shows the values of σ and τ as functions of θ (the angle between the normal to a plane and the principal stress direction, σ_1.

Figure 5.7-6: Definition of the Coulomb-Mohr failure criterion.